

This is an Open Access document downloaded from ORCA, Cardiff University's institutional repository:<https://orca.cardiff.ac.uk/id/eprint/164678/>

This is the author's version of a work that was submitted to / accepted for publication.

Citation for final published version:

Tucciarelli, Raffaele, Ejaz, Naveed, Wesselink, Daan B., Kolli, Vijay, Hodgetts, Carl J., Diedrichsen, Jörn and Makin, Tamar R. 2023. Does ipsilateral remapping following hand loss impact motor control of the intact hand? *The Journal of Neuroscience* 10.1523/JNEUROSCI.0948-23.2023

Publishers page: <http://dx.doi.org/10.1523/JNEUROSCI.0948-23.2023>

Please note:

Changes made as a result of publishing processes such as copy-editing, formatting and page numbers may not be reflected in this version. For the definitive version of this publication, please refer to the published source. You are advised to consult the publisher's version if you wish to cite this paper.

This version is being made available in accordance with publisher policies. See <http://orca.cf.ac.uk/policies.html> for usage policies. Copyright and moral rights for publications made available in ORCA are retained by the copyright holders.



Research Articles | Development/Plasticity/Repair

## Does ipsilateral remapping following hand loss impact motor control of the intact hand?

<https://doi.org/10.1523/JNEUROSCI.0948-23.2023>

Received: 23 May 2023

Revised: 31 October 2023

Accepted: 21 November 2023

Copyright © 2023 Tucciarelli et al.

This is an open-access article distributed under the terms of the [Creative Commons Attribution 4.0 International license](#), which permits unrestricted use, distribution and reproduction in any medium provided that the original work is properly attributed.

---

*This Early Release article has been peer reviewed and accepted, but has not been through the composition and copyediting processes. The final version may differ slightly in style or formatting and will contain links to any extended data.*

**Alerts:** Sign up at [www.jneurosci.org/alerts](http://www.jneurosci.org/alerts) to receive customized email alerts when the fully formatted version of this article is published.

1 Does ipsilateral remapping following hand loss impact motor control  
2 of the intact hand?  
3

4 Raffaele Tucciarelli<sup>1,2</sup>, Naveed Ejaz<sup>3</sup>, Daan B. Wesselink<sup>4,5</sup>, Vijay Kolli<sup>6</sup>, Carl J. Hodgetts<sup>7,8</sup>, Jörn  
5 Diedrichsen<sup>3,9</sup>, Tamar R. Makin<sup>1,2,4</sup>

6 <sup>1</sup>MRC Cognition & Brain Sciences Unit, Cambridge, England, United Kingdom; <sup>2</sup>Institute of Cognitive Neuroscience,  
7 University College London, London, UK; <sup>3</sup>Departments of Statistical and Actuarial Sciences, and Computer Science, Western  
8 University, London, Ontario, CA; <sup>4</sup>WIN Centre, Nuffield Department of Clinical Neuroscience, University of Oxford, Oxford,  
9 UK; <sup>5</sup>Department of Neurobiology, Harvard Medical School, USA; <sup>6</sup>Queen Mary's Hospital, London, United Kingdom;  
10 <sup>7</sup>CUBRIC, School of Psychology, Cardiff University, UK; <sup>8</sup>Royal Holloway University of London, Egham, UK; <sup>9</sup>Brain and Mind  
11 Institute, Western University, London, Ontario, CA.

12

13 **Corresponding authors:**

14 Tamar R. Makin

15 Professor of Cognitive Neuroscience

16 Wellcome Trust Senior Research Fellow

17 E: [tamar.makin@mrc-cbu.cam.ac.uk](mailto:tamar.makin@mrc-cbu.cam.ac.uk)

18 T: +44 (0)1223 767661

19 W: [www.plasticity-lab.com](http://www.plasticity-lab.com)

20

21 Raffaele Tucciarelli

22 Post-doctoral researcher

23 MRC CBU, University of Cambridge, 15 Chaucer Rd, Cambridge CB2 7EF

24 ICN, University College London (UCL), Alexandra House, 17-19 Queen Square, London WC1N 3AZ

25 E1: [Raffaele.Tucciarelli@mrc-cbu.cam.ac.uk](mailto:Raffaele.Tucciarelli@mrc-cbu.cam.ac.uk)

26 E2: [r.tucciarelli@ucl.ac.uk](mailto:r.tucciarelli@ucl.ac.uk)

27

28 The authors declare no competing financial interests

29

## Abstract

What happens once a cortical territory becomes functionally redundant? We studied how the brain and behaviour change for the remaining hand in humans (male and female) with either a missing hand from birth (one-handers) or due to amputation. Previous studies reported that in amputees, but not in one-handers, there is increased ipsilateral activity in the somatosensory territory of the missing hand (i.e., remapping). We used a complex finger task to explore whether this observed remapping in amputees involves recruiting more neural resources to support the intact hand to meet greater motor control demand. Using basic fMRI analysis, we found that only amputees had more ipsilateral activity when motor demand increased, however this did not match any noticeable improvement in their task performance. More advanced multivariate fMRI analysis showed that amputees had stronger and more typical representation – relative to controls' contralateral hand representation – compared to one-handers. This suggests that in amputees, both hand areas work together more collaboratively, potentially reflecting the intact hand's efference copy. One-handers struggled to learn difficult finger configurations, but this did not translate to differences in univariate or multivariate activity relative to controls. Additional white matter analysis provided conclusive evidence that the structural connectivity between the two hand areas did not vary across groups. Together, our results suggest that enhanced activity in the missing hand territory may not reflect intact hand function. Instead, we suggest that plasticity is more restricted than generally assumed and may depend on the availability of homologous pathways acquired early in life.

**Key words:** fingers; fMRI; hand; primary motor cortex; primary somatosensory cortex; motor control; acquired amputees; one-handers; brain plasticity

## Significant Statement

People with congenital hand absence (one-handers) and amputees rely on their intact hand for everyday actions. This extensive daily training could result in increased motor ability, supported by neural resources within the missing-hand territory (i.e., ipsilateral to the intact hand). However, using a demanding multi-finger configuration task, we observed reduced sensorimotor learning in one-handers in the most difficult configuration. Furthermore, despite increased ipsilateral activity, amputees did not show superior intact hand motor ability. Multivariate fMRI analyses suggested a collaborative relationship between the contralateral and ipsilateral hand territories of amputees, which was unique compared to the other two groups. These results suggest that brain plasticity is limited and may depend on the availability of homologous pathways acquired early in life.

## Author contributions

T.R.M., J.D. and N.E. designed research; T.R.M., D.B.W., N.E., and V.K. performed research; R.T., C.J.H., D.B.W., and N.E. analysed data; R.T. and T.R.M. wrote the first draft of the paper; All authors edited the paper.

# 1 Introduction

2 Specific functions of mature cortical areas are determined by their molecular properties, histological  
3 organization, and connectional fingerprints. The unique identity of a given area is determined by  
4 genetic expression and is moderated by electrical activity over the course of early development (see  
5 Sur and Rubenstein, 2005 for review). This phase of increased susceptibility to input in shaping the  
6 neural circuit is called a *critical period* (Levelt and Hübener, 2012). The critical period might be  
7 enabled because of plasticity ‘brakes’, such as inhibitory circuits, neural over-growth and synaptic  
8 pruning, normally affording homeostatic balance, have not yet been finalised (Takesian and Hensch,  
9 2013). Yet, even in these earliest stages of development, it seems that the assignment of brain  
10 function to a given cortical structure is largely fixed. For example, fMRI studies of children with left  
11 hemisphere perinatal stroke found that the (typically left dominant) language areas in the inferior  
12 frontal cortex were located in anatomically homologous areas in the right hemisphere (Tillema et al.,  
13 2008; Raja Beharelle et al., 2010; Tuckute et al., 2022). In this context, it is interesting to consider  
14 how a redundant cortical area’s function changes after hand loss, either because of congenital hand  
15 malformation (hereafter – one-handers) or acquired arm amputation later in life (hereafter –  
16 amputees).

17 Extensive research has mainly explored neighbouring body part homunculus ‘remapping’ following  
18 hand loss (see Muret and Makin, 2021 for review), with a focus on the face (Pons et al., 1991; Flor et  
19 al., 1995; Raffin et al., 2016). However, from a functional perspective, the intact hand is expected to  
20 gain the most from redundant resources in the missing hand territory to adapt to life with only one  
21 hand. If this reallocation of resources from the missing hand territory towards the intact hand is  
22 functional, and if brain plasticity is more potent in early development, we should find improved  
23 motor abilities and learning in one-handers relative to controls. Surprisingly, while the deprived  
24 hand area of one-handers was demonstrated to be activated by multiple body parts (e.g. arm, face,  
25 feet, torso), it does not appear to be activated by the intact hand (Hahamy et al., 2017; Hahamy and  
26 Makin, 2019). Instead, previous research reported increased activity in the missing hand territory  
27 from the (ipsilateral) intact hand in amputees (Kew et al., 1994; Hamzei et al., 2001; Bogdanov et al.,  
28 2012; Makin et al., 2013a; Philip and Frey, 2014; Valyear et al., 2020). Thus, bimanual experience  
29 might be required to establish a functional connection between the two hands to enable ipsilateral  
30 functionality (Philip et al., 2015), but direct evidence supporting this is limited. Moreover, previous  
31 studies used *basic* motor tasks (e.g., opening and closing the hand, moving a single digit). If  
32 ipsilateral processing due to plasticity processes provides *additional* resources to aid motor control  
33 of the intact hand, it may require difficult tasks to activate it. Similarly, prior results were primarily  
34 inferred from net activity changes in the hand territory, under the (potentially naïve) assumption  
35 that greater activity reveals greater functional involvement. However, as demonstrated in recent  
36 learning studies (Berlot et al., 2020) multivariate approaches provide a more detailed opportunity to  
37 establish changes in functional brain representation.

38 Here we aimed to address the relationship between brain and behavioural adaptations for the intact  
39 hand in individuals with a missing hand. To better gauge whether activity changes in one-handers  
40 and amputees are functional, we varied task difficulty. Participants had to simultaneously press with  
41 three fingers onto a piano-like keyboard, while keeping the other two fingers relaxed. Some  
42 combination of fingers are known to be more difficult than others (Waters-Metenier et al., 2014),  
43 and we therefore selected two sets of 5 configurations that systematically ranged from easy to  
44 difficult. Motor difficulty is known to increase activity level, particularly in the ipsilateral hemisphere  
45 (Verstynen et al., 2005). Therefore, we used brain scans while participants performed the same task

46 to compare the net activity (remapping) and multivariate representational similarity (information  
47 content and representational structure) of the missing and intact hand territories. While we provide  
48 results from the primary somatosensory and motor territories (S1 and M1), we focus our research  
49 on S1, which has been the historical primary culprit for remapping following amputation-related  
50 deprivation (Merzenich et al., 1984; Pons et al., 1991). S1 is also known to contain greater  
51 information content relating to finger movements (Ejaz et al., 2015; Berlot et al., 2019; Arbuckle et  
52 al., 2022), and plays a crucial role for dexterous hand control (Brochier et al., 1999) and motor  
53 planning (Ariani et al., 2022). To explore the structural underpinnings of these functional changes,  
54 we also used diffusion MRI to examine potential white matter microstructural changes in  
55 transcallosal fibre connections linking the two hand areas.

56 We predicted that, if one-handers rely on ipsilateral processing for difficult tasks, we should see  
57 increased activity and information content in the missing hand cortex compared to controls, leading  
58 to improved performance compared to controls. Alternatively, if the functional availability of  
59 homologous resources depends on bimanual experience, we should expect to find greater activity  
60 and information content in the missing hand territory of amputees relative to controls. Moreover,  
61 this information should be organised in a homologous representational structure relative to the  
62 intact hand territory.

## 63 Materials and Methods

64 The experimental procedures described in this manuscript were run as part of a larger study (the full  
65 study protocol can be found on <https://osf.io/gmvua/>). Here we focus on procedures related to the  
66 finger coordination task. The motor task was similar to previous studies (Waters-Metenier et al.,  
67 2014; Ejaz et al., 2015). Participants took part in the training session outside the scanner first and  
68 then an fMRI session.

### 69 *Participants*

70 Amputees (N=19; 4 females; Mean Age=49.05±12.05), one-handers (N=16; 9 females; Mean  
71 Age=43.44±11.40), and two-handed controls (N=16; 7 females; Mean Age=45.37±10.67) were  
72 invited to take part in a motor control task. The current experiment was comprised of a training  
73 session outside the scanner, followed by a scanning session. Not all participants were able to take  
74 part in (or complete) the scanning session. Thus, the final sample in the scanning session was N=16  
75 amputees (4 females; Mean Age=48.40±12.6), N=13 one-handers (7 females; Mean  
76 Age=45.80±11.30), and N=14 two-handed controls (5 females; Mean Age=44.20±12.20).  
77 Furthermore, due to technical reasons, we could not register the responses of two amputee  
78 participants in the scanner, therefore the analyses of the finger coordination task during the MRI  
79 session were based on N=14 amputees (2 females; Mean Age=49.5±13.1). For the DTI, we were able  
80 to collect data for N=18 amputees, N=13 one-handers, and N=13 controls. Three of the amputee  
81 participants lost their dominant hand. However, considering they were amputated for at least 26  
82 years, their non-dominant hand had effectively taken on the role of dominance. Table 1 displays the  
83 demographic information of the participants. The mean age was not significantly different between  
84 groups (Motor training:  $F_{(2,48)}=1.10$ ,  $p=.341$ ,  $\eta_p=.034$ ; Scanner session:  $F_{(2,39)}=1.11$ ,  $p=.340$ ,  $\eta_p=.054$ ).  
85 Nevertheless, to take into account any potential inter-individual impact of age, we included  
86 participants' age as a covariate in the analyses. In all analyses, outliers were defined as values  
87 exceeding the metrics of interest of three standard deviations from the mean. We made a pre-  
88 determined decision to retain all data points, including those considered outliers, as long as their  
89 removal would not have caused any qualitative changes to the results. For the behavioural data  
90 during the training session, we identified one potential outlier, but since this outlier did not impact  
91 the results qualitatively, we opted to include the outlier in the final analysis. For the multivariate  
92 data, we identified an outlier that we decided to remove because its removal qualitatively changed  
93 the significance level.

94 Recruitment was carried out in accordance with the University of Oxford's Medical Sciences inter-  
95 divisional research ethics committee (MS-IDREC-C2-2015-012). Informed consent and consent to  
96 publish was obtained in accordance with ethical standards set out by the Declaration of Helsinki. All  
97 participants were compatible with local magnetic resonance imaging (MRI) safety guidelines.

### 98 *Apparatus*

99 Responses were recorded using a custom-built 5-finger MRI-compatible piano-like device (Wiestler  
100 and Diedrichsen, 2013; Ejaz et al., 2015; Wesselink et al., 2019). Each key was equipped with a  
101 sensor that could continuously measure isometric force during a finger press. The sensors were  
102 connected to a laptop and the applied forces were monitored online. Participants received real-time  
103 visual feedback on how much force each finger exerted by means of moving horizontal white cursors  
104 corresponding to each key. In the training task outside the scanner, the apparatus was placed on a  
105 desk in front of the seated participant, who rested the five fingers of their intact hand (or dominant  
106 hand in controls) on the keys that were immobile but able to measure the applied pressure.  
107 Participants could choose to keep their fingers extended or flexed, based on comfort. Inside the



108 scanner, the device was placed on their lap or belly, depending on their preference. Ensuring  
109 participants' comfort was paramount in this experiment because we wanted them to be able to  
110 control their fingers during a complex task (i.e., the finger configuration task). This is standard  
111 practise both inside and outside the scanner.

JNeurosci Accepted Manuscript

112 *General procedure*

113 *Instructions:* The top of the screen showed five vertical grey bars, each corresponding to one of the  
114 keys. At rest, participants were required to apply and maintain a minimal force (0.5N) on the keys, as  
115 indicated by a horizontal bar at the bottom of the screen (hereafter baseline area). In a typical trial,  
116 three of the vertical bars turned green indicating which of the keys to press. Participants were  
117 instructed to wait until the appearance of a go cue that was provided as a green horizontal bar  
118 similar in dimension and right above the baseline area. At this point, participants had to press three  
119 keys in synchrony (chord-like configuration) and using the same force (2.5N) on all instructed fingers  
120 while keeping the non-instructed fingers placed relaxed on the keys. In this way, participants had to  
121 use the sensory information provided by all fingers which is fundamental in dexterous manipulation  
122 (Pruszynski et al., 2016). Participants received a positive feedback (i.e., a point) as soon as they  
123 configured the instructed fingers as required. Once the finger cursors were successfully stabilised in  
124 the target area, the area disappeared indicating the participants to go back to the baseline position  
125 (this was a requirement to obtaining a point in the next trial) by releasing the pressure on the  
126 instructed fingers. At this point, a new trial started. Note that the training session was self-paced,  
127 whereas the scanning session was timed (see below for details).

128 *Training session:* First, the experimenter explained the task and showed the participants how to use  
129 the device. Then, the participants performed a few familiarization trials with a set of configurations  
130 not used in the study. This was followed by a single-finger movement block, where the participants  
131 had to press only one of the five fingers. This block was repeated one more time at the end of the  
132 training (as detailed in Wesselink et al., 2019). Then, the actual training session started and it lasted  
133 25 minutes. Within this time window, participants were encouraged to complete as many blocks as  
134 possible. Each block was about 3 minutes-long, depending on the performance, leading to a variable  
135 number of blocks across participants. On average, participants completed  $M_{all}=5.69$  blocks  
136 ( $SD_{all}=1.42$ ;  $M_{Amputees}= 5.58$ ,  $SD_{Amputees}= 1.54$ ;  $M_{One-handers}= 5.62$ ,  $SD_{One-handers}= 1.36$ ;  $M_{Controls}= 5.87$ ,  
137  $SD_{Controls}= 1.41$ ), and the three groups did not differ for the number of blocks completed  
138 ( $F_{(2,48)}=0.20$ ,  $p=.817$ ,  $\eta_p=.01$ ). Visual instructions of the required chord were presented for 3 seconds,  
139 followed by the go cue. Within each block, instructions for the same finger configuration were  
140 repeated 4 times.

141 *fMRI session:* After the training session, participants were invited to take part in a similar motor task  
142 as part of the fMRI study. In the scanner, there was no minimal pressure requirement at baseline  
143 because the application of constant pressure was tiring while lying supine. In addition, the task was  
144 timed. Visual instructions were presented for 1.3 seconds, and participants had to execute the chord  
145 (i.e., press and release the keys) within 2.3 seconds from the onset of the instructions. The same  
146 instruction was repeated three time resulting in blocks of 6.9 seconds. Each finger configuration  
147 block was repeated three times within a run, resulting in 45 trials per run (9 trials by 5 finger  
148 configurations). Participant took part in four runs and each run lasted around 3.5 minutes (141  
149 volumes).

150 *Behavioral performance:* Behavioural performance was measured as the deviance from the required  
151 finger configuration, by taking into account two sources of error: 1) any deviation of the non-  
152 instructed fingers from the baseline (0.5 N); and 2) any deviation of the each instructed fingers from  
153 the average force as all the instructed fingers were expected to exert a similar force (2.5 N). These  
154 two forms of residuals were computed within the response and release time, summed up and  
155 averaged across time to obtain a unique measure of performance per trial (see Waters-Metenier et  
156 al., 2014). In line with previous studies (Ejaz et al., 2015; Waters et al., 2017), the beginning of the

157 response was defined as the point in time in which at least one of the fingers exceeded the  
158 threshold of 1.5 N when pressed.

### 159 *Finger configuration and difficulty levels*

160 Figure 1 displays the configurations used in the training session (Panel A, easy to difficult from the  
161 bottom to the top) and in the scanner (Panel D, easy to difficult from the bottom to the top). In the  
162 training session, we used the following finger configurations (1: Thumb, 2: Index, 3: Middle, 4: Ring,  
163 5: Little finger): 345, 123, 124, 245, 135. The aim of the training session was twofold: 1) measure the  
164 sensorimotor learning of participants, and 2) familiarise participants with the task before entering  
165 the scanner. In the scanner, we used different finger configurations (145, 234, 134, 125, and 235) in  
166 order to minimise any differences across groups that were hypothesised to arise due to different  
167 training capacity.

168 To independently confirm the previously estimated difficulty levels of finger configurations, defined  
169 from a pilot session of a previous study (Waters-Metenier et al., 2014), were appropriately labelled,  
170 we also utilized a model-based approach. To this aim, we used the amount of flexion enslavement  
171 (% of maximal voluntary contraction) between fingers in a single-finger task (Yu et al., 2010). In  
172 particular, considering the task's complexity that involves simultaneous control of multiple digits, we  
173 reasoned that difficulty is influenced by at least three components: easy configurations would be  
174 characterised by high amount of enslavement between instructed fingers (component 1) and non-  
175 instructed fingers (component 2), and low amount of enslavement between the instructed and non-  
176 instructed fingers (component 3). In other words, it is easier to move in parallel fingers with high  
177 amount of enslavement, as it is to keep relaxed fingers with high amount of enslavement.  
178 Furthermore, it is easier to control a finger configuration where the instructed and non-instructed  
179 fingers have low amount of enslavement. More specifically, for each chord, we estimated the three  
180 components of enslavement as follow: the total (i.e., sum) of enslavement for the instructed fingers  
181 (E1), the enslavement for the non-instructed fingers (E2), and the enslavement between the  
182 instructed and non-instructed fingers (E3). Then, we combined the three components (i.e., E1+E2-  
183 E3) to obtain a unique measure of enslavement such that the configurations with a high score were  
184 categorized as easier than the ones with a low score. Using this measure, we sorted the  
185 configurations from easy to difficult and divided them into two groups: *easy* (345, 145, 234, 123,  
186 124) and *difficult* (134, 125, 245, 235, 135). In our analysis, for the training session, the *easy*  
187 averaged configurations were 345, 123, and 124, and the *difficult* averaged configurations were 245  
188 and 135; for the scanning session, the *easy* averaged configurations were 145 and 234, and the  
189 *difficult* averaged configurations were 134, 125, and 235. We also used this scoring to establish the  
190 easiest and most difficult configurations for specific fMRI analysis.

### 191 *MRI data acquisition*

192 MRI images were acquired using a 3T MAGNETON Prisma MRI scanner (Siemens, Erlangen,  
193 Germany) with a 32-channel head coil. Functional images were collected using a multiband T2\*-  
194 weighted pulse sequence with a between-slice acceleration factor of 4 and no in-slice acceleration (2  
195 mm isotropic, TR: 1500 ms), covering the entire brain. The following acquisition parameters were  
196 used: TE: 32.40 ms; flip angle: 75°, 72 transversal slices. Field maps were acquired for field  
197 unwarping. A T1- weighted sequence was used to acquire an anatomical image (TR: 1900 ms, TE:  
198 3.97 ms, flip angle: 8°, spatial resolution: 1 mm isotropic). Diffusion-weighted MRI (dMRI) data were  
199 acquired using the following parameters: TR: 2951 ms, TE: 79.80 ms, flip angle: 80°, spatial  
200 resolution: 1.5 mm isotopic, 84 transversal slices. Gradients were applied along 60 uniformly  
201 distributed directions with a b-value of 1000 s/mm<sup>2</sup>. Five non-diffusion-weighted images with b = 0  
202 s/mm<sup>2</sup> were also acquired. No task was given to the participants during the structural and DTI

203 acquisition. They viewed a calm nature video to prevent them from falling asleep and making large  
204 head movements.

### 205 *fMRI preprocessing and first-level analysis*

206 MRI data were preprocessed using a standard pipeline as implemented in FSL 6 (Smith et al., 2004;  
207 Jenkinson et al., 2012). The following steps were applied to each functional run: motion correction  
208 using MCFLIRT (Jenkinson et al., 2002); B0 fieldmap correction to account from distortions due to  
209 magnetic field inhomogeneity; brain extraction using BET (Jenkinson et al., 2002); high-pass  
210 temporal filtering of 90 s; and spatial smoothing with a Gaussian kernel of full with at half maximum  
211 (FWHM) of 5 mm for the univariate analyses and 3 mm for the multivariate analyses.

212 In order to estimate brain activity related to our configuration task, we employed a voxel-based  
213 general linear model (GLM) as implemented in FEAT. For each functional run, time series were  
214 predicted using five regressors of interest corresponding to the five configurations that participants  
215 had to do in the scanner. These regressors were convolved with a double-gamma function and their  
216 temporal regressors were also added to the design matrix to account for temporal variability of the  
217 BOLD response. We also included the motion parameters resulting from the MCFLIRT step, and  
218 columns indicating outlier volumes as returned from the FSL function *fsl\_motion\_outliers* with  
219 default and recommended parameters (root mean square intensity difference of each volume to the  
220 reference volume as metric; as a threshold, metrics that were larger than 75<sup>th</sup>  
221 percentile+1.5\*InterQuartile range were considered outliers). The number of volume outliers was  
222 small for all groups (Amputee group: mean proportion volumes excluded= 0.044±0.012; One-  
223 handers group: mean proportion volumes excluded= 0.045± 0.017; Control group: mean proportion  
224 volumes excluded= 0.047±0.019), and there was no difference between the three groups ( $F_{(2,40)}=$   
225 0.152,  $p=.860$ ,  $\eta_p=.008$ ).

### 226 *MRI analysis*

227 For each individual, cortical surfaces were estimated from the structural images using Freesurfer  
228 5.3.0 (Dale et al., 1999; Fischl et al., 2001). To define the ROIs, we used the Brodmann Area (BA)  
229 maps included in Freesurfer (Fischl et al., 2008) that are based on the histological analysis of ten  
230 human post-mortem brains. We used the Connectome Workbench software  
231 (<https://www.humanconnectome.org/software/connectome-workbench>) to visualise the surfaces  
232 and to ensure accurate spatial registration between the structural and functional volumes, as well as  
233 to verify the precise alignment of the ROIs. Connectome Workbench was also used to map the  
234 volumetric maps to the surface space.

### 235 *ROI definition*

236 Since our main aim was to investigate brain plasticity following hand loss, we focused our analyses  
237 on bilateral hand S1 (and area BA3b in particular), which has been most commonly associated with  
238 remapping in animal and human studies (see Makin and Flor, 2020 for a literature overview).  
239 Conversely, M1 has typically been considered relatively unchanged following amputation. This is  
240 mainly due to the fact that while sensory input is lost, motor output remains preserved, forming the  
241 basis for myoelectric prosthetics and brain-computer interfaces. Further motivation for our S1 focus  
242 is that previous research has consistently shown that S1 contains more finger information (including  
243 inter-finger configurations) relative to M1 (Schieber and Hibbard, 1993; Ejaz et al., 2015). This is  
244 because S1 topography tends to be well-defined, relative to M1 where the information content is  
245 more widespread (Schieber, 2001; Graziano and Aflalo, 2007; Berlot et al., 2019; Arbuckle et al.,  
246 2022). Lastly, sensory feedback has a crucial role in shaping task demands and therefore the  
247 relevance of S1 to our task becomes evident. However, we also report results from M1 (area BA4)

248 for completeness. The ROIs were defined in the fsaverage template space using probabilistic  
249 cytoarchitectonic maps (Fischl et al., 2008), based on 2.5 cm proximal/distal (Wiestler and  
250 Diedrichsen, 2013; Berlot et al., 2019; Ogawa et al., 2019; Arbuckle et al., 2022) to the hand knob  
251 (Yousry et al., 1997). The resulting hand S1 was then projected to the individual reconstructed  
252 surfaces. Here we focused on nodes with at least 50% probability of being part of BA3b. We chose  
253 this threshold to make sure that all of BA3b was included, and to make sure the regions were large  
254 enough. However, we note that given the inherent smoothness of the data, our preprocessing  
255 procedure and the probabilistic nature of the anatomical atlas, the ROIs are likely to contain relevant  
256 activity from neighbouring S1 areas. We then mapped the surface ROIs to the individual volumetric  
257 high-resolution anatomy and resampled to the lower resolution functional brain. Hand M1 was  
258 defined in a similar way as hand S1 described above. As a control region, we used hMT+ that was  
259 created combining area FST, V4t, MT and MST from the Human Connectome Project parcellation  
260 (Glasser et al., 2016).

### 261 *Representational similarity analysis (RSA)*

262 Information content within each ROI was estimated using RSA (Kriegeskorte et al., 2008). For each  
263 participant and run, we extracted the first-level betas estimated with FEAT (see previous section  
264 *fMRI preprocessing and first-level analysis*) from each ROI and computed the pairwise cross-  
265 validated Mahalanobis (or crossnobis) distance (Walther et al., 2016) between chord-related beta  
266 patterns as a measure of their dissimilarity. Multidimensional noise normalisation was used to  
267 increase reliability of distance estimates (noisier voxels are down-weighted), based on the voxel's  
268 covariance matrix calculated from the GLM residuals. The advantage of using the crossnobis distance  
269 is twofold: 1) spatially correlated noise is removed using multivariate noise normalization and this  
270 improves the estimate of the dissimilarities (Walther et al., 2016); 2) cross-validation ensure that if  
271 two patterns only differ by noise, their mean dissimilarity estimate will be zero. As a consequence,  
272 the dissimilarity between two patterns can also be negative (Diedrichsen et al., 2016) and thus  
273 dissimilarities significantly larger than zero can be taken as evidence that the two patterns are  
274 distinct and that the ROI contain task-related information (e.g., distinct representation of  
275 configurations). The crossnobis dissimilarity was computed using the python library for RSA  
276 *rsatoolbox* version 0.0.4 (<https://github.com/rsagroup/rsatoolbox>).

### 277 *Diffusion MRI preprocessing*

278 Diffusion data were preprocessed using a custom pipeline that combined tools from MRITrix 3.0  
279 (Tournier et al., 2019), ExploreDTI 4.8.6 (Leemans et al., 2009), and FSL 5.0.9 (Smith et al., 2004;  
280 Jenkinson et al., 2012). These included: 1) de-noising using the MP-PCA (principal component  
281 analysis of Marchenko-Pastur) method in MRITrix (Veraart et al., 2016); 2) Gibbs ringing correction  
282 using 'mrdegibbs' in MRITrix (partial Fourier; Kellner et al., 2016); 3) Global signal drift correction  
283 using ExploreDTI (Vos et al., 2017); and 4) Motion EPI distortion correction using Eddy and Topup  
284 within FSL (Andersson et al., 2003). Data were visually checked as part of quality assurance  
285 procedures. Whole brain voxel-wise maps of fractional anisotropy (FA) and mean diffusivity (MD)  
286 maps were then derived from the preprocessed data by fitting the diffusion tensor model. FA  
287 represents the degree to which diffusion is constrained in a particular direction, and ranges from 0  
288 (isotropic diffusion) to 1 (anisotropic diffusion). MD ( $10^{-3}\text{mm}^2\text{s}^{-1}$ ) represents the average diffusivity  
289 rate. The diffusion tensor was estimated and fitted using the nonlinear least squares method with  
290 Robust Estimation of Tensors by Outlier Rejection (RESTORE) applied (Chang et al., 2005).

### 291 *Tractography*

292 A multiple-ROI tractography approach enabled specific transcallosal pathways to be constructed in  
293 each participant between their left and right S1 hand areas (see also Postans et al., 2020). Initially,

294 each participant’s ROIs in T1 space (see Section *ROI definition* above) were registered to their native  
 295 space diffusion MRI image using the following steps: 1) the T1-to-diffusion transformation matrix  
 296 was generated using FLIRT with 6 degrees-of-freedom and the correlation ratio cost function. The  
 297 fractional anisotropy (FA) map was used as the reference image (rather than the b0 image) as it  
 298 provided better image contrast; 2) the transformation matrix was then applied to the individual  
 299 subject ROIs in T1 space using FLIRT. As tractography can be challenging from grey matter ROIs (due  
 300 to low anisotropy), the diffusion space ROIs were dilated by 1.5 mm to include some white matter  
 301 voxels (Thomas et al., 2014).

302 Tractography was initially performed from all voxels in the left hemisphere ROI in each participant’s  
 303 native diffusion MRI space in ExploreDTI (v4.8.3; Leemans et al. 2009) using a deterministic  
 304 tractography algorithm based on constrained spherical deconvolution (Tournier et al. 2008;  
 305 Jeurissen et al. 2011). Spherical deconvolution approaches enable multiple peaks to be extracted in  
 306 the fibre orientation density function within a given voxel, allowing complex fibre arrangements,  
 307 such as crossing/kissing fibres, to be modelled more accurately (Dell’Acqua and Tournier, 2019). The  
 308 contralateral S1 ROI was then used as an “AND” gate to capture any streamlines that arose from the  
 309 seed ROI and terminated in the contralateral ROI. Next, the same procedure was repeated, this time  
 310 starting with the right hemisphere ROI as seed and gating with the right hemisphere. This process  
 311 was conducted for each participant and then inspected visually by the research team (CJH, RT). A  
 312 step size of 0.1 mm and an angle threshold of 60° were applied to prevent the reconstruction of  
 313 anatomically implausible streamlines. Tracking was performed with a supersampling factor of 4 × 4 ×  
 314 4 (i.e., streamlines were initiated from 64 grid points, uniformly distributed within each voxel). The  
 315 resulting inter-hemispheric pathways were then intersected with the whole-brain voxel-wise FA and  
 316 MD maps (see above) to derive four tract-specific measures of microstructure in each participant  
 317 (S1-to-S1 and M1-to-M1, in both directions). As in Postans et al. (2020), the FA and MD values for  
 318 the left-to-right and right-to-left segments were combined into a streamline-weighted mean using  
 319 the following equation:

$$320 \quad \text{Vertex - Weighted Mean FA} = \frac{(N_{L \rightarrow R} \times \overline{FA_{L \rightarrow R}}) + (N_{R \rightarrow L} \times \overline{FA_{R \rightarrow L}})}{(N_{L \rightarrow R} + N_{R \rightarrow L})}$$

$$321 \quad \text{Vertex - Weighted Mean MD} = \frac{(N_{L \rightarrow R} \times \overline{MD_{L \rightarrow R}}) + (N_{R \rightarrow L} \times \overline{MD_{R \rightarrow L}})}{(N_{L \rightarrow R} + N_{R \rightarrow L})}$$

322

### 323 *Tract-based spatial statistics (TBSS)*

324 We also conducted a complementary voxel-wise statistical analysis of the FA and MD data using  
 325 TBSS (Smith et al., 2006). First, each participant’s FA and MD maps were aligned to the standard MNI  
 326 template using nonlinear registration (Andersson et al., 2010). Second, the mean FA image was  
 327 created and subsequently thinned (using the default FA threshold = 0.2) to generate the mean FA  
 328 skeleton, which represents the centre of all tracts common to the group. Third, participants’ FA and  
 329 MD data were projected onto the skeleton for voxel-wise analyses using randomise in FSL (Winkler  
 330 et al., 2014). For both FA and MD, a general linear model was constructed, which specified contrasts  
 331 between amputees and one-handers (amputees > one-handers, and one-handers > amputees), and  
 332 also each experimental group against controls. Age (de-meaned) was added as a covariate.  
 333 Following prior work (Hahamy et al., 2015), analyses were first restricted to the bilateral  
 334 corticospinal tract using an ROI mask [labelled “WM Corticospinal tract”] from the Julich Histological  
 335 Atlas (Amunts et al., 2020) using threshold free cluster enhancement (TFCE) with a corrected alpha

336 of 0.05. We also conducted an additional whole brain analysis to examine any potential group  
337 difference outside our main ROIs (using the same TFCE- corrected threshold of  $p = 0.05$ ). All reported  
338 TBSS co-ordinates are in MNI 152 space.

### 339 *Statistical analysis*

340 Statistical analyses were performed using custom-made scripts written in Matlab R2020b (The  
341 MathWorks), R version 4.1.3 (R Core Team, 2022) with RStudio (2021.09.0 Build 351), python 3.10.6  
342 with spyder 5.3.3, and JASP 0.17. Behavioural performance (mean deviation) for the training and the  
343 scanning sessions were analysed using three-way repeated-measures ANCOVAs (rmANCOVAs) with  
344 age (de-meaned) included as a covariate, group as a between-subject factor, and block number and  
345 difficulty as within-subject factors. Brain activity (z scores, averaged across runs) for each ROI was  
346 analysed using a three-way rmANCOVA with age included as a covariate, group as a between-subject  
347 factor, and hemisphere and difficulty as within-subject factors. To test for existing information  
348 content, dissimilarities were tested against zeros using a two-tailed one-sample t-test for each group  
349 and hemisphere. Dissimilarities were also analysed in two ways. In one analysis, we only selected the  
350 easiest and most difficult finger configuration pairs and used a three-way rmANCOVA with age  
351 included as a covariate, group as a between-subject factor, and hemisphere and difficulty as within-  
352 subject factors. In a second analysis, we averaged across all finger configuration pairs and ran a two-  
353 way rmANCOVA with age included as a covariate, group as a between-subject factor, and  
354 hemisphere as a within-subject factor. To test for existing functional homotopy (i.e., correlation  
355 between finger configuration pairs across hemispheres), we used two-tailed one-sample t-test for  
356 each group and hemisphere. We also used a one-way ANCOVA with age as a covariate and group as  
357 a between-subject factor to investigate differences in functional homotopy between groups. To  
358 investigate similarity to typical contralateral representation in the experimental groups (i.e.,  
359 correlation between the RDMs of the experimental participants, amputees and one-handers, with  
360 the contralateral RDM averaged across the control participants), we used two-tailed one-sample t-  
361 test for each group and hemisphere. We also used a two-way rmANCOVA with age as a covariate,  
362 group (one-handers, amputees) as a between-subject factor, and hemisphere as a within-subject  
363 factor to investigate differences in typical contralateral representation between the experimental  
364 groups. Prior to these analyses, correlation values were standardized using the Fisher's r-to-z  
365 transformation. Independent t-tests were used to test for group differences. The experimental  
366 groups (amputees and one-handers) were compared against the control group unless differently  
367 specified. To control for age while performing an independent t-test, we first ran an ANCOVA and  
368 then computed the contrasts of interest using the R package *emmeans* 1.8.2. For post-hoc  
369 comparisons that were exploratory (that is, not a priori and not confirmatory), we adjusted our  
370 significance alpha level for multiple-comparisons using the Bonferroni approach. In the results  
371 section, we report the uncorrected p-values with a note of the adjusted alpha level. For non-  
372 significant results of interest, we reported the corresponding Bayes Factor ( $BF_{10}$ ), defined as the  
373 relative support for the alternative hypothesis. While it is generally agreed that it is difficult to  
374 establish a cut-off for what consists sufficient evidence, we used the threshold of  $BF < 1/3$  as  
375 sufficient evidence in support of the null, consistent with others in the field (Wetzels et al., 2011;  
376 Dienes, 2014). For Bayesian ANCOVAs, we used a uniform model as a prior and for Bayesian t-tests,  
377 we used the Cauchy model with a width of 0.707, which are the default settings in JASP. For all  
378 analyses, whenever the normality assumptions were not met, we adopted a permutation approach  
379 using the function *aovperm* of the R package *permuco* 1.1.2 with default settings (permutation  
380 method for fixed effects models: *freedman\_lane*; for mixed effects models:  
381 *Rd\_kheradPajouh\_renaud*) and we report these results with a note only when they are qualitatively  
382 different from the parametric approach.

383 *Data code and accessibility*

384 The preprocessed data and the scripts necessary to reproduce the analyses can be found at  
385 <https://osf.io/hsvkc/>.

## 386 Results

### 387 One-handers show reduced benefits from brief training of difficult finger configurations

388 We first explored whether individuals with a missing hand, either due to congenital malformation  
389 (one-handers) or amputation in adulthood (amputees), differ from controls in their ability to learn to  
390 perform a finger configuration task with varying levels of difficulty. Mean deviations from the  
391 instructed hand configuration for each of the 5 configurations across the first 7 blocks are shown for  
392 the three groups in Figure 1B, with more difficult configurations displayed in cooler colours. At the  
393 first attempt (block 1), there was no difference in performance between the experimental and  
394 control groups, except for a trend for the most difficult level, in which one-handers showed worse  
395 performance compared to the control group (10 comparisons, no corrections for multiple  
396 comparisons). To quantify training effects across groups, we averaged deviation means between  
397 easy (configurations 1-2) and difficult levels (configurations 3-5) for each participant, and compared  
398 performance between the first and last blocks completed during training (Figure 1C). The resulting 3  
399 (group) x 2 (block) x 2 (difficulty) ANCOVA (controlling for age) resulted in a significant 3-way  
400 interaction ( $F_{(2,47)}=5.28$ ,  $p=.009$ ,  $\eta_p=0.18$ ), indicating that participants across the 3 groups benefited  
401 differently from the practice, with respect to difficulty levels. In addition, a main effect of difficulty  
402 ( $F_{(1,47)}=137.22$ ,  $p<.001$ ,  $\eta_p=0.74$ ) and block number ( $F_{(1,47)}=17.48$ ,  $p<.001$ ,  $\eta_p=0.27$ ) was found, with  
403 no significant main effect of group ( $F_{(2,47)}=1.31$ ,  $p=.280$ ,  $\eta_p=0.05$ ). As apparent from the figures, this  
404 was driven by a lack of learning effect in the one-handed group, specifically for the difficult  
405 configurations. To better quantify this, we ran a separate repeated-measures ANCOVA for each  
406 group and observed a significant interaction between block number and difficulty for the one-  
407 handers only ( $F_{(1,14)}=12.61$ ,  $p=.003$ ,  $\eta_p=0.47$ ). To further explore the differential learning effect  
408 observed in the one-handed group, we compared differences in performance between the last and  
409 the first block (Figure 1C), and found a significant learning effect in the easy condition only (Easy:  
410  $t_{(14)}=-3.58$ ,  $p=.003$ ; Difficult:  $t_{(15)}=.14$ ,  $p=.889$ ,  $BF_{10}=0.258$ ; Bonferroni adjusted  $\alpha: .05/2=.025$ ),  
411 suggesting that the impairment in learning was specific for the difficult configurations. This was also  
412 confirmed by significant differences in the last block of training between one-handers and controls  
413 for the difficult configurations only ( $t_{(47)}=2.32$ ,  $p=.024$ ).

414 We next examined whether these group differences in performance were replicated in the fMRI  
415 task, where 5 different configurations were used Figure 1D. Figure 1E shows performance across the  
416 4 runs. To test for differential learning effects, we repeated the analysis mentioned above while  
417 comparing performance across groups and difficulty levels between the first and the last runs (Figure  
418 1F). The 3-way interaction in the ANCOVA was not significant ( $F_{(2,38)}=.48$ ,  $p=.622$ ,  $\eta_p=0.02$ ), indicating  
419 that the groups did not show different learning effects – indeed as shown in the figure, performance  
420 had already plateaued. However, we did observe a significant interaction between group and  
421 difficulty ( $F_{(2,38)}=3.93$ ,  $p=.028$ ,  $\eta_p=0.17$ ), indicating that participants in different groups responded  
422 differently to task difficulty. We also observed a trend towards a main effect of group ( $F_{(2,38)}=2.71$ ,  
423  $p=.080$ ,  $\eta_p=0.12$ ), in addition to a main effect of difficulty ( $F_{(1,38)}=73.61$ ,  $p<.001$ ,  $\eta_p=0.66$ ) and block  
424 number ( $F_{(1,38)}=9.89$ ,  $p=.003$ ,  $\eta_p=0.21$ ). The interaction between group and difficulty only showed a  
425 trending result and was driven by the one-handers performing worse on the difficult configurations  
426 relative to controls ( $t_{(38)}=2.38$ ,  $p=.022$ , Bonferroni adjusted  $\alpha: .05/3=.0167$ ). This is reflective of the  
427 behavioural results found outside the scanner, where the one-handers showed worst performance



428 on the difficult configurations at the end of the training session. Here, we also found a trending  
429 result suggesting performance deficits in the amputee group relative to controls in the difficult  
430 configurations ( $t_{(38)}=2.42$ ,  $p=.021$ , Bonferroni adjusted  $\alpha: .05/3=.0167$ ). However, the one-hander  
431 and amputees groups did not differ relative to each other in performance ( $t_{(38)}=0.06$ ,  $p=.955$ ,  
432 Bonferroni adjusted  $\alpha: .05/3=.0167$ ). It is important to note that previous tests comparing the two  
433 experimental groups against the control group only showed a trend (i.e., did not survive the multiple  
434 comparisons correction as the Bonferroni corrected p-values were both below .067), and as such,  
435 these findings should be interpreted with caution.

436

### 437 **Amputees show increased averaged ipsilateral activity that scales with difficulty**

438 Next, we examined univariate activity levels across the bilateral S1 hand regions of interest (ROIs,  
439 Figure 2A). To estimate whether difficulty modulated brain activity differently for the different  
440 groups and hemispheres, we first conducted a 3-level ANCOVA, including 3 (group) x 2 (hemisphere)  
441 x 2 (difficulty) and age (as a covariate). We observed a significant 3-way interaction  
442 ( $F_{(2,39)}=5.23$ ,  $p=.010$ ,  $\eta_p=0.21$ ), confirming that difficulty modulates activity differently across  
443 hemispheres and groups, as shown in Figure 2B. The analysis also revealed a significant interaction  
444 between group and hemisphere ( $F_{(2,39)}=6.46$ ,  $p=.004$ ,  $\eta_p=0.25$ ), difficulty and hemisphere  
445 ( $F_{(1,39)}=6.16$ ,  $p=.018$ ,  $\eta_p=0.14$ ), and main effects of hemisphere ( $F_{(1,39)}=71.02$ ,  $p<.001$ ,  $\eta_p=0.65$ ) and  
446 difficulty ( $F_{(1,39)}=11.33$ ,  $p=.002$ ,  $\eta_p=0.23$ ). To further explore the 3-way interaction, we conducted two  
447 separate 2-level ANCOVAs for each hemisphere. As hypothesised, we observed group differences  
448 within the ipsilateral cortex only, where we found a significant interaction between group and  
449 difficulty ( $F_{(2,39)}=3.39$ ,  $p=.044$ ,  $\eta_p=0.15$ ) and a main effect of group ( $F_{(2,39)}=5.95$ ,  $p=.006$ ,  $\eta_p=0.23$ ),  
450 while no main effect or interaction involving group was observed in the contralateral hemisphere (all  
451  $p>.6$ ). This suggests that activity scales with task difficulty differently across groups in the ipsilateral  
452 cortex (which is the missing hand cortex in the experimental groups). The main effect of difficulty  
453 was significant in both hemispheres (Contralateral:  $F_{(1,39)}=15.68$ ,  $p<.001$ ,  $\eta_p=0.287$ ; Ipsilateral:  
454  $F_{(1,39)}=5.57$ ,  $p=.023$ ,  $\eta_p=0.125$ ). The ipsilateral interaction between group and difficulty was driven by  
455 an increase of activity with difficulty in the amputees ( $t_{(39)}= 3.55$ ,  $p<.001$ ), but not in one-handers or  
456 controls ( $t_{(39)}=-0.18$ ,  $p=.857$ ;  $t_{(39)}= 0.90$ ,  $p=. 373$ ). Furthermore, amputees showed significantly larger  
457 activity than controls in the ipsilateral cortex for both the difficult ( $t_{(39)}= 3.37$ ,  $p=.002$ ) and the easy  
458 conditions ( $t_{(39)}= 3.22$ ,  $p=.003$ ). Together, these findings confirm and extend previous studies –  
459 ipsilateral activity for the intact hand was heightened in amputees, particularly with increased task  
460 difficulty. Conversely, the one-handed group did not show any significant benefit or disadvantage in  
461 activating the missing hand cortex relative to controls.

462 We repeated the same analysis in bilateral M1 hand ROI (Figure 4B). The 3-way interaction was not  
463 significant in this case ( $F_{(2,39)}=1.50$ ,  $p=.236$ ,  $\eta_p=0.07$ ). We observed a significant interaction between  
464 difficulty and hemisphere ( $F_{(1,39)}=11.48$ ,  $p=.002$ ,  $\eta_p=0.23$ ), driven by activity increase with difficulty in  
465 the contralateral hemisphere only (Contralateral:  $t_{(39)}=4.07$ ,  $p=.0002$ ; Ipsilateral:  $t_{(39)}=2.02$ ,  $p=.05$ ,  
466 Bonferroni adjusted  $\alpha: .05/2=.025$ ). We also observed a significant interaction between group and  
467 hemisphere ( $F_{(2,39)}=4.83$ ,  $p=.013$ ,  $\eta_p=0.20$ ), due to the fact that the difference in activity between the  
468 two hemispheres was reduced in the amputees relative to the control groups ( $t_{(39)}= -3.05$ ,  $p=0.004$ ,  
469 Bonferroni adjusted  $\alpha: .05/3=.0167$ ). This is in line with the observation that the amputees showed  
470 higher activity in the ipsilateral hemisphere than the control group. We did not find main effects or  
471 interaction between group and difficulty (all  $p>.3$ ). Overall, these results suggest that contrary to  
472 ipsilateral S1, ipsilateral M1 does not scale with difficulty in the amputees. Finally, to confirm that  
473 our effects reflect increased difficulty relating to motor performance per se, rather than more

474 general task demands, e.g. relating to attentional or arousal effects, we repeated the same analysis  
475 in a control visual region (left and right hMT+; Figure 4E) and observed no significant main effects or  
476 interactions (all  $p > .11$ ).

477

#### 478 Amputees show bilateral increase in information content relative to one-handers

479 We next assessed whether the selective increase in unilateral activity observed in amputees,  
480 previously interpreted as functional remapping, translated to a gain in information content. Average  
481 distances (across all configuration pairs as shown in Figure 3A) were significantly greater than zero  
482 (all  $p < .05$ , not corrected for multiple comparisons), confirming that task relevant information was  
483 encoded in both hemispheres. We first examined distances by specifically comparing the easy and  
484 difficult configurations separately across hemispheres and groups. To allow us to specifically account  
485 for difficulty, this analysis was restricted to the easiest configuration pair (C234-C145) and the most  
486 difficult configuration pair (C235-C125) in our representational dissimilarity matrix (highlighted in  
487 Figure 3A, green: easiest; blue: most difficult). If increase in activity translate to information content  
488 gain, we should see larger distances between configuration pairs for the amputees, especially across  
489 the most difficult conditions. However, we did not find a significant 3-way interaction  
490 ( $F_{(2,38)}=0.41$ ,  $p=.668$ ,  $\eta_p=0.15$ ), or a resulting 2-way interaction involving group (see Figure 2C).  
491 Instead, we found a main effect of group ( $F_{(2,38)}=3.29$ ,  **$p=.048$** ,  $\eta_p=0.15$ ) driven by increased  
492 information content in amputees relative to one-handers ( $t_{(38)}= 2.55$ ,  **$p=.015$** , Bonferroni adjusted  $\alpha$ :  
493  $.05/3=.0167$ ). We also observed a main effect of hemisphere ( $F_{(1,38)}=15.57$ ,  **$p<.001$** ,  $\eta_p=0.29$ ) and  
494 difficulty ( $F_{(1,38)}=11.91$ ,  **$p=.001$** ,  $\eta_p=0.24$ ). Interestingly, we found that information scales down with  
495 difficulty, regardless of group, suggesting that the overall increase in information observed in  
496 amputees is not linked to their reduced performance.

497 To take best advantage of our information content analysis, we repeated the analysis while  
498 comparing the average distances across the entire RDM (10 cells) across groups and hemispheres in  
499 a 2-way ANCOVA. Again, if increase in activity translate to information content gain, we should see  
500 larger averaged distance between configuration pairs for the amputees. Here again, we found no  
501 significant interaction ( $F_{(2,38)}=0.65$ ,  $p=.525$ ,  $\eta_p=0.03$ ), suggesting that information content was not  
502 modulated differently across group and hemisphere. Instead, again, we found a main effect of group  
503 ( $F_{(2,38)}=3.83$ ,  **$p=.030$** ,  $\eta_p=0.17$ ) and hemisphere ( $F_{(1,38)}=25.84$ ,  **$p<.001$** ,  $\eta_p=0.40$ ). The main effect of  
504 group was again driven by increased distances across both hemispheres in amputees relative to one-  
505 handers ( $t_{(38)}= 2.62$ ,  **$p=.013$** ). Similar to the previous analysis, these effects were not specific to the  
506 ipsilateral cortex, but were instead generalised. Do these group differences reflect increased  
507 information in amputees or decreased information in one-handers? When comparing against  
508 controls, the results are ambiguous (amputees versus controls:  $t_{(38)}= 1.99$ ,  $p=.054$ ,  $BF_{10}=0.90$ ; one-  
509 handers versus controls:  $t_{(38)}= -0.57$ ,  $p=.573$ ,  $BF_{10}=0.46$ ; Bonferroni adjusted  $\alpha$ :  $0.05/2=.025$ ).  
510 Together, it appears that the increased activity found in the ipsilateral hemisphere of amputees for  
511 the difficult configurations does not neatly translate to a selective increased information content.

512 To further confirm the specificity of our effects, we repeated the same analyses in M1 and hMT+,  
513 and verified that the averaged distances were also significantly larger than zero (all  $p < .007$ , not  
514 corrected for multiple comparisons). In M1 (Figure 4C), when focusing on difficulty as a factor, we  
515 observed a main effect of difficulty ( $F_{(1,38)}=5.60$ ,  **$p=.023$** ,  $\eta_p=0.13$ ), suggesting larger distances  
516 between the easiest pairs than the most difficult ones, and hemisphere ( $F_{(1,38)}=15.83$ ,  **$p<.01$** ,  
517  $\eta_p=0.29$ ), suggesting larges distances in the contralateral hemisphere relative to the ipsilateral  
518 hemisphere. No main effect of group ( $F_{(2,38)}=2.05$ ,  $p=.143$ ,  $\eta_p=0.10$ ), and no group interactions (group

519 x hemisphere:  $F_{(2,38)}=0.44$ ,  $p=.648$ ,  $\eta_p=0.023$ ; group x difficulty:  $F_{(2,38)}=0.50$ ,  $p=.610$ ,  $\eta_p=0.026$ .  
520 Similarly, when averaging across all configurations, we observed a main effect of hemisphere  
521 ( $F_{(1,38)}=14.79$ ,  $p<.001$ ,  $\eta_p=0.28$ ), suggesting larger distances in the contralateral relative to the  
522 ipsilateral hemisphere, no main effect of group ( $F_{(2,38)}=1.94$ ,  $p=.158$ ,  $\eta_p=0.09$ ), and no group  
523 interactions ( $F_{(2,38)}=0.18$ ,  $p=.836$ ,  $\eta_p=0.000$ ). Despite higher distances in hMT+ (presumably due to  
524 the visual information provided throughout the motor task; Figure 4F), we did not observe any main  
525 effects or interactions (all  $p > 0.2$ ).

526

## 527 Amputees show increased functional homotopy in representational structure across 528 hemispheres

529 Functional homotopy refers to brain regions in opposite hemispheres exhibiting correlated activity  
530 patterns during a task or at rest, and suggests that two brain regions are functionally associated and  
531 working in concert to perform a certain function (e.g., a motor task). We explored the degree of  
532 functional homotopy (defined here as the correlation between the representational dissimilarity  
533 matrices shown in Figure 3A) in the hand region across the two hemispheres. We first correlated the  
534 10 configuration pairs of the RDM across the two S1 hand areas of each participant. The homotopy  
535 correlation values were significantly larger than zero for the amputee and one-hander groups, but  
536 not for the controls (Amputees:  $t_{(15)}=2.83$ ,  $p=.013$ ; One-handers:  $t_{(12)}=3.28$ ,  $p=.006$ ; Controls:  $t_{(12)}=-$   
537  $0.59$   $p=.563$ ,  $BF=0.32$ ; Bonferroni adjusted  $\alpha: .05/3=.016$ ). When comparing across groups (using a 1-  
538 way ANCOVA, accounting for age), we found a trend towards significance ( $F_{(2,38)}=2.99$ ,  $p=.062$ ,  
539  $\eta_p=.14$ ,  $BF_{10}=2.05$ ), which is also reflected in greater homotopy in amputees relative to controls  
540 ( $t_{(38)}=2.41$ ,  $p=.021$ ), but not for one-handers relative to controls ( $t_{(38)}=1.63$ ,  $p=.112$ ,  $BF_{10}=1.44$ ;  
541 Bonferroni adjusted  $\alpha: .05/2=.025$  for the last 2 comparisons).

542 To determine whether the increased homotopy found in amputees reflects typical contralateral  
543 representation of the ipsilateral (missing hand) cortex, we next compared the ipsilateral  
544 representational structure of amputees and one-handers to the average RDM of controls'  
545 contralateral averaged RDM (see "Typical contralateral representation" in Figure 3C). As shown in  
546 Figure 3C, for amputees we found a significant (above zero) correlation between both contralateral  
547 and ipsilateral ROIs relative to the typical contralateral representational structure in controls  
548 (Amputees Contralateral:  $t_{(15)}=6.82$ ,  $p<.001$ ; Amputees Ipsilateral:  $t_{(15)}= 4.38$ ,  $p<.001$ , one-sample t-  
549 test; Bonferroni adjusted  $\alpha: 0.05/2=0.025$ ), whereas the correlation between one-handers and  
550 controls was approaching significance for the contralateral ROI only (One-handers contralateral:  
551  $t_{(12)}=2.51$ ,  $p=.027$ ; One-handers ipsilateral:  $t_{(12)}=1.70$ ,  $p=.114$ ; Bonferroni adjusted  $\alpha: 0.05/2=0.025$ ).  
552 The two-way ANCOVA comparing group and hemisphere showed an expected effect of hemisphere  
553 ( $F_{(1,26)}=9.44$ ,  $p=.005$ ,  $\eta_p=0.26$ ), reflecting the greater correlation of the contralateral hemisphere, and  
554 a significant main effect of group ( $F_{(1,26)}= 4.64$ ,  $p=.041$ ,  $\eta_p=0.15$ ). The interaction was not significant  
555 ( $F_{(1,26)}=1.73$ ,  $p=.20$ ,  $\eta_p=0.06$ ). This demonstrates that amputees represented the different finger  
556 configurations bilaterally in way that was similar to the typical representation in the contralateral  
557 hemisphere in neuro-typical controls.

558 When repeating the same set of analyses in M1, amputees only showed a significant correlation  
559 between the contralateral ROI relative to the typical contralateral structure in controls (Amputees  
560 Contralateral:  $t_{(15)}=2.81$ ,  $p=.013$ ; Amputees Ipsilateral:  $t_{(15)}= 0.45$ ,  $p=.659$ ; Bonferroni adjusted  $\alpha:$   
561  $0.05/2=0.025$ ; One-handers Contralateral:  $t_{(12)}= 1.62$ ,  $p=.131$ ; One-handers Ipsilateral:  $t_{(12)}= 0.57$ ,  
562  $p=.575$ ; Bonferroni adjusted  $\alpha: 0.05/2=0.025$ ). Furthermore, the two-way ANCOVA revealed a

563 significant main effect of hemisphere ( $F_{(1,26)}=5.55$ ,  $p=.026$ ,  $\eta_p=0.17$ ), no main effect of group ( $F_{(1,26)}=$   
564  $0.04$ ,  $p=.840$ ,  $\eta_p=0.02$ ) and no interaction ( $F_{(1,26)}=0.61$ ,  $p=.443$ ,  $\eta_p=.02$ ).

#### 565 No differences in white matter tracts between the three groups

566 Finally, we analysed diffusion MRI data, collected in the same cohort, to explore whether the group  
567 differences observed in the functional analysis are also reflected by alterations in structural  
568 connectivity. As noted in the Introduction, it is possible that ipsilateral functionality depends on the  
569 brain establishing (through bimanual experience) a functional interaction between the two hand  
570 territories. One possibility is that this is mediated, at least in part, via transcallosal pathways that  
571 connect the two hand areas (Fling et al., 2013). To address this, we conducted deterministic  
572 tractography to examine potential differences in the tissue microstructural properties of the  
573 transcallosal fibres connecting the two hand areas. We first compared the vertex-weighted mean FA  
574 and MD, derived from tractography-based inter-hemispheric connections, using two separate  
575 ANCOVAs (controlling for age). For both metrics, the main effect of group was not significant (FA:  
576  $F_{(2,35)}=0.05$ ,  $p<.950$ ,  $\eta_p=.003$ ,  $BF_{10}=0.19$ ; MD:  $F_{(2,35)}=0.08$ ,  $p<.922$ ,  $\eta_p=.005$ ,  $BF_{10}=0.20$ ). The Bayes  
577 Factors in both analyses provided evidence in favour of the null hypothesis being no group structural  
578 differences in FA and MD.

579 To explore potential differences between amputees/one-handers and controls beyond these  
580 transcallosal interhemispheric connections, we conducted a complementary voxel-wise TBSS  
581 analyses at the whole brain level, as well as within a corticospinal tract ROI (see Methods; Hahamy  
582 et al., 2015). At the whole brain level, we found no FA or MD differences between either group  
583 (amputees and one-handers) or controls (TFCE-corrected,  $p=0.05$ ). We also saw no significant  
584 clusters when contrasting amputees with one-handers. We did, however, find a negative effect of  
585 age, confirming the quality of the data. For the corticospinal tract, we similarly found no significant  
586 differences between each experimental group and the controls (both FA and MD), and this was also  
587 the case when comparing amputees with one-handers. Together, these findings do not support  
588 substantial structural changes in white matter architecture most relevant for inter-hemispheric  
589 coordination for motor control in our experimental groups.

## 590 Discussion

591 In this study, we investigated the impact of hand loss, whether congenital or through amputation, on  
592 motor ability and intact hand representation. Given the profound behavioural pressure of growing  
593 up and/or living with only one hand, perceptual learning combined with practice effects are likely to  
594 enhance motor skills of the intact hand in both groups. Critical development periods may be more  
595 favourable for training effects to occur (Sur and Rubenstein, 2005; Levelt and Hübener, 2012),  
596 favouring plasticity in one-handers and thus improving motor control and learning of the intact  
597 hand. Instead, we found that one-handers showed poorer performance in a finger configuration  
598 task, particularly when learning more difficult configurations, whereas amputees did not show any  
599 clear deviations from controls during task training outside the scanner. This aligns with prior  
600 research indicating motor deficits in one-handers but not amputees. For example, one-handers  
601 (Philip et al., 2015) but not amputees (Philip and Frey, 2011) exhibited accuracy and speed deficits  
602 while planning a grasp with their intact hand. Based on this, it has been postulated that  
603 sensorimotor experience of both hands is necessary for the refinement of accurate unilateral motor  
604 prediction and performance (Philip et al., 2015). Relatedly, we previously found that one-handers  
605 made more errors during visually guided reaching with their artificial arm, relative to amputees, as  
606 well as two-handed controls using their nondominant arm (Maimon-Mor et al., 2021) (though it is  
607 worth noting that in this study intact hand reaching performance was not significantly different from  
608 the other groups). Interestingly, one-handers who started using an artificial arm earlier in life as  
609 toddlers showed less motor deficit, hinting at a critical period for integrating a visuomotor  
610 representation of a limb. These findings imply that early-life disabilities may impede motor  
611 development, even for body parts not directly affected by the malformation. This does not  
612 necessarily contradict the prediction that motor control and learning would be superior in one-  
613 handers due to early-life behavioural pressure. It is possible that critical periods trigger both long-  
614 term deficits and improved skill that would counterbalance each other. Without early-life over-  
615 practice, one-handers would show more severe motor impairments in their daily life.

616 Although the missing hand territory showed increased activity during the task (as discussed below),  
617 amputees did not display superior motor performance with their intact hand. The idea of amputees  
618 gaining enhanced abilities following their amputation due to reallocation of central resources in the  
619 missing hand cortex has been a topic of much fascination for the past century. Originally, hypotheses  
620 (and reports) focused on heightened tactile sensitivity on the residual limb (stump) of human  
621 amputees (e.g., Katz, 1920; Teuber, H and Krieger, HP and Bender, 1949; Haber, 1955) (see Makin,  
622 2021 for maladaptive consequences of reorganisation in amputees). Merzenich and colleagues  
623 (1984) proposed that remapping following finger amputation should improve tactile acuity of the  
624 neighbouring fingers. Other studies, using short-term and reversible deafferentation, suggested  
625 increased acuity for the non-deafferented ('intact') hand due to increased excitability of the  
626 deafferented hemisphere (Björkman et al., 2004; Lissek et al., 2009; Dempsey-Jones et al., 2019).  
627 More recently, we and other suggested that increased activity for the intact hand in the missing  
628 hand territory is a potential neural correlate of adaptive plasticity for motor abilities (Makin et al.,  
629 2013a; Philip and Frey, 2014). According to these ideas, the brain can correctly interpret missing  
630 hand territory signals as related to the intact hand, thereby providing greater (or better) information  
631 about the new representation. This is consistent with physiological studies showing that, while hand  
632 and finger movements are mostly controlled through contralateral (crossed) corticospinal  
633 projections (Brinkman and Kuypers, 1973), there are also known ipsilateral (uncrossed) motor  
634 projections (Soteropoulos et al., 2011). Given that amputees rely heavily on their remaining hand,  
635 one might expect improved read-out of neural signals originating from the ipsilateral cortex, which

636 typically has limited functionality in two-handed individuals. This improvement should lead to  
637 recruitment of the missing hand hemisphere in the brain's ipsilateral region. However, much of the  
638 original evidence for perceptual gains in amputees have been since challenged (O'Boyle et al., 2001;  
639 Vega-Bermudez and Johnson, 2002). In our brief training paradigm, we found no evidence for motor  
640 behavioural benefits in amputees.

641 What is then the functional relevance of the increased ipsilateral activity observed in sensorimotor  
642 cortex of amputees here, as well as in many previous studies (Kew et al., 1994; Hamzei et al., 2001;  
643 Bogdanov et al., 2012; Makin et al., 2013a; Philip and Frey, 2014; Valyear et al., 2020)? One difficulty  
644 in interpreting the functional meaning of net changes in activity levels is that they could result from  
645 multiple dissociated mechanisms, such as aberrant processing (Makin et al., 2013b), disinhibition  
646 (Hahamy et al., 2017), or merely reflect gain changes due to upstream processing (Kambi et al.,  
647 2014). Common to these alternative processes is that increased activity doesn't necessarily entail a  
648 change of the underlying information being processed (Arbuckle et al., 2019). In other words,  
649 activity changes that underlie remapping do not necessarily entail information content changes. In  
650 the present study, we found that, while difficulty increases contralateral activity across all groups, in  
651 the ipsilateral cortex difficulty increases activity significantly only in amputees. This is interesting,  
652 because it goes against the idea that the increased ipsilateral activity is a simple passive  
653 consequence of inter-hemispheric disinhibition (Werhahn et al., 2002; Ramachandran and  
654 Altschuler, 2009; Simões et al., 2012). Instead, amputees selectively recruited the ipsilateral cortex  
655 for more difficult configurations. However, this does not necessarily indicate functional recruitment  
656 of ipsilateral cortex. Representational similarity analysis (RSA) is a multivariate technique designed  
657 to determine how separate or distinct one activity pattern is to another. RSA allows us to ask not  
658 only if more information is available in a given brain area (dissimilarity distances), but also whether  
659 this new information is structured consistently with known representational principles, e.g. related  
660 to the contralateral hemisphere. By quantifying and characterising brain function beyond the spatial  
661 attributes of activity maps, while providing a more precise model for how information content varies  
662 across configurations, we believe RSA provides an arguably better tool for assessing the functional  
663 characteristics of the ipsilateral cortex. Furthermore, both in our previous study (conducted on the  
664 same set of participants Wesselink et al., 2019) and here, we found that the increased activity in  
665 amputees did not translate to differentially increased ipsilateral information.

666 Several previous studies using multivariate pattern analysis have demonstrated that, despite activity  
667 suppression, ipsilateral sensory and motor cortex contains information pertaining to individual  
668 fingers (Diedrichsen et al., 2013b, 2018; Berlot et al., 2019; Wesselink et al., 2019). These ipsilateral  
669 activity patterns appear to be weaker, but otherwise similar in representational structure to those  
670 elicited by movement of the mirror-symmetric finger in the opposing hand, at least for single finger  
671 movements (Diedrichsen et al., 2013a, 2018). The ipsilateral representation is not a simple 'spill-  
672 over' or passive copy from the homologous (contralateral) hand area, as it has been shown to be  
673 differently modulated by behavioural task context (Berlot et al., 2019). Yet, the functional  
674 significance of these ipsilateral representations and independence from the contralateral  
675 representation is still unknown. Ipsilateral activity in M1 has also been observed in monkey studies  
676 during proximal (i.e., shoulders and elbows) motor tasks (Ames and Churchland, 2019; Heming et al.,  
677 2019; Cross et al., 2020). These studies seem to suggest that, even if the same population of neurons  
678 encodes both ipsilateral and contralateral movements, the two limb representations are distributed  
679 differently across neurons (i.e., arm-related activity occupies distinct subspaces), which is proposed  
680 to be the mechanism that avoid impacting (i.e., moving) the wrong arm. Furthermore, it has been  
681 suggested that the ipsilateral representation is an *efference* copy resulting from the contralateral  
682 activity to inform the ipsilateral cortex about the contralateral arm movement and help with

683 bimanual coordination (Ames and Churchland, 2019). The efference copy would be sent by default,  
684 even in the absence of bimanual movements, and ignored if not needed. In other words, the  
685 ipsilateral representation could be a consequence of the fact that the two homologous areas inform  
686 each other about their respective current state. Although the relationship between level of task  
687 complexity and the functional role of the efference copy has not been explored yet, it is interesting  
688 to speculate that the relevance of the efference copy will be greater for tasks requiring coordination  
689 across hands.

690 This latter interpretation provides an interesting conceptual framework for our reported findings: in  
691 one-handers, limited bimanual experience will dampen the mechanistic development of bimanual  
692 hand representation, including cross-hemisphere efference copy, reducing bilateral information  
693 content. Instead, in amputees, the ipsilateral efference copy from the intact hand will be more  
694 prominent in the missing hand cortex due to the reduced utilisation of the missing hand, resulting in  
695 increased homotopy for the intact hand across the two hemispheres. Importantly, under this  
696 conceptual framework, these representational changes do not necessarily impact behaviour because  
697 the efference copy is presumably involved in improving bimanual coordination, which is impossible  
698 for amputees to implement. This interpretation is consistent with a recent study which did not find a  
699 functional relevance for increased S1 ipsilateral activity (Valyear et al., 2020), in line with our  
700 observation that amputees did not show any behavioural improvement outside the scanner and, if  
701 anything, they showed a performance reduction inside the scanner. Our white matter findings also  
702 indirectly support the idea that activity changes are functional irrelevant, as they reveal stable  
703 anatomy despite increased activity and better inter-hemispheric collaboration. In this context, it is  
704 interesting to consider previous evidence for persistent representation of the missing hand in  
705 amputees (Raffin et al., 2012; Makin et al., 2013b). The intact hand's homotopic representation in  
706 the missing hand cortex might help maintain the missing hand representation. While we and others  
707 previously showed that the phantom hand map is activated by phantom hand movements  
708 independently of the intact hand (Kikkert et al., 2016; Bruurmijn et al., 2017; Wesselink et al., 2019),  
709 it is still possible that structured inputs from the intact hand (via ipsilateral pathways) sustains the  
710 missing hand map, despite the loss of the original peripheral inputs.

711 As potential limitations, we did not control for variations in finger postures, device locations, and  
712 hand sizes, which could influence task complexity. For example, since the device was unique,  
713 participants with smaller hands might have found the task more complicated than participants with  
714 larger hands. While we acknowledge the potential impact of these factors, we believe none of them  
715 had a significant impact on our results. Participants were allowed to choose their preferred device  
716 position and finger postures based on comfort, aiming to optimize their performance. Furthermore,  
717 the finger device was designed with elongated keys similar to a piano. In our experience this design  
718 accommodates a broad range of hand sizes. Although we didn't collect explicit hand size data, we  
719 used gender as a proxy, assuming women generally have smaller hands. Even after including gender  
720 in our models, the results remained consistent.

721 To conclude, our findings reveal a collaborative relationship between contralateral and ipsilateral  
722 cortices during task performance in amputees. By focusing on information content and its  
723 representational structure above and beyond the salient effects of remapping, defined as increased  
724 mean activity, our findings highlight a different aspect of the critical period than normally  
725 emphasised, which is based on experience rather than deprivation. Specifically, representations of  
726 both hands and some bimanual experience in the early developmental stage is necessary to develop  
727 a bilateral motor representation and a typical contralateral representation. Interestingly, while the  
728 ipsilateral efference copy interpretation is functionally irrelevant for the unimanual tasks studied

729 here and in previous research, it may provide a useful consideration, and perhaps even exciting new  
730 opportunities, for combining novel restorative brain-computer interfaces (Fouad et al., 2015) and  
731 augmentation technologies (Dominijanni et al., 2021) for bimanual interactions.

## 732 **Acknowledgments**

733 Funding was provided by the Wellcome Trust (215575/Z/19/Z) and the Medical Research Council  
734 (MC\_UU\_00030/10) awarded to T.R.M. We thank our participants and Opcare for their help and  
735 commitment, Fiona van den Heiligenberg, Lucilla Cardinali and Harriet Dempsey-Jones for help with  
736 data collection. For the purpose of open access, the author has applied a Creative Commons  
737 Attribution (CC BY) licence to any Author Accepted Manuscript version arising from this submission.

JNeurosci Accepted Manuscript



## References

- Ames KC, Churchland MM (2019) Motor cortex signals for each arm are mixed across hemispheres and neurons yet partitioned within the population response. *Elife* 8:1–36.
- Amunts K, Mohlberg H, Bludau S, Zilles K (2020) Julich-Brain: A 3D probabilistic atlas of the human brain's cytoarchitecture. *Science* (80- ) 369:988–992.
- Andersson JLR, Jenkinson M, Smith S (2010) Non-linear registration, aka spatial normalization (FMRIB technical report TR07JA2). FMRIB Anal Gr Univ Oxford.
- Andersson JLR, Skare S, Ashburner J (2003) How to correct susceptibility distortions in spin-echo echo-planar images: Application to diffusion tensor imaging. *Neuroimage* 20:870–888.
- Arbuckle SA, Pruszynski JA, Diedrichsen J (2022) Mapping the Integration of Sensory Information across Fingers in Human Sensorimotor Cortex. *J Neurosci* 42:5173–5185 Available at: <https://www.jneurosci.org/lookup/doi/10.1523/JNEUROSCI.2152-21.2022>.
- Arbuckle SA, Yokoi A, Pruszynski JA, Diedrichsen J (2019) Stability of representational geometry across a wide range of fMRI activity levels. *Neuroimage* 186:155–163.
- Ariani G, Pruszynski JA, Diedrichsen J (2022) Motor planning brings human primary somatosensory cortex into action-specific preparatory states. *Elife* 11:1–20.
- Berlot E, Popp NJ, Diedrichsen J (2020) A critical re-evaluation of fmri signatures of motor sequence learning. *Elife* 9:1–24.
- Berlot E, Prichard G, O'Reilly J, Ejaz N, Diedrichsen J (2019) Ipsilateral finger representations in the sensorimotor cortex are driven by active movement processes, not passive sensory input. *J Neurophysiol* 121:418–426.
- Björkman A, Rosén B, Van Westen D, Larsson EM, Lundborg G (2004) Acute improvement of contralateral hand function after deafferentation. *Neuroreport* 15:1861–1865.
- Bogdanov S, Smith J, Frey SH (2012) Former hand territory activity increases after amputation during intact hand movements, but is unaffected by illusory visual feedback. *Neurorehabil Neural Repair* 26:604–615.
- Brinkman J, Kuypers HGJM (1973) CEREBRAL CONTROL OF CONTRALATERAL AND IPSILATERAL ARM, HAND AND FINGER MOVEMENTS IN THE SPLIT-BRAIN RHESUS MONKEY. *Brain* 96:653–674 Available at: <https://academic.oup.com/brain/article-lookup/doi/10.1093/brain/96.4.653>.
- Brochier T, Boudreau M-J, Paré M, Smith AM (1999) The effects of muscimol inactivation of small regions of motor and somatosensory cortex on independent finger movements and force control in the precision grip. *Exp Brain Res* 128:31–40 Available at: <http://link.springer.com/10.1007/s002210050814>.
- Bruurmijn MLCM, Pereboom IPL, Vansteensel MJ, Raemaekers MAH, Ramsey NF (2017) Preservation of hand movement representation in the sensorimotor areas of amputees. *Brain* 140:3166–3178.
- Chang LC, Jones DK, Pierpaoli C (2005) RESTORE: Robust estimation of tensors by outlier rejection. *Magn Reson Med* 53:1088–1095.
- Cross KP, Heming EA, Cook DJ, Scott SH (2020) Maintained Representations of the Ipsilateral and Contralateral Limbs during Bimanual Control in Primary Motor Cortex. *J Neurosci* 40:6732–6747 Available at: <https://www.jneurosci.org/lookup/doi/10.1523/JNEUROSCI.0730-20.2020>.

- Dale AM, Fischl B, Sereno MI (1999) Cortical Surface-Based Analysis: I. Segmentation and Surface Reconstruction. *Neuroimage* 9:179–194 Available at: <https://linkinghub.elsevier.com/retrieve/pii/S1053811998903950>.
- Dell'Acqua F, Tournier JD (2019) Modelling white matter with spherical deconvolution: How and why? *NMR Biomed* 32:1–18.
- Dempsey-Jones H, Themistocleous AC, Carone D, Ng TWC, Harrar V, Makin TR (2019) Blocking tactile input to one finger using anaesthetic enhances touch perception and learning in other fingers. *J Exp Psychol Gen* 148:713–727 Available at: <http://doi.apa.org/getdoi.cfm?doi=10.1037/xge0000514>.
- Diedrichsen J, Provost S, Zareamoghaddam H (2016) On the distribution of cross-validated Mahalanobis distances. *arXiv Prepr*:1–24 Available at: <http://arxiv.org/abs/1607.01371>.
- Diedrichsen J, Wiestler T, Ejaz N (2013a) A multivariate method to determine the dimensionality of neural representation from population activity. *Neuroimage* 76:225–235 Available at: <http://dx.doi.org/10.1016/j.neuroimage.2013.02.062>.
- Diedrichsen J, Wiestler T, Krakauer JW (2013b) Two distinct ipsilateral cortical representations for individuated finger movements. *Cereb Cortex* 23:1362–1377.
- Diedrichsen J, Yokoi A, Arbuckle SA (2018) Pattern component modeling: A flexible approach for understanding the representational structure of brain activity patterns. *Neuroimage* 180:119–133 Available at: <https://linkinghub.elsevier.com/retrieve/pii/S1053811917306985>.
- Dienes Z (2014) Using Bayes to get the most out of non-significant results. *Front Psychol* 5:1–17.
- Dominijanni G, Shokur S, Salvietti G, Buehler S, Palmerini E, Rossi S, De Vignemont F, D'Avella A, Makin TR, Prattichizzo D, Micera S (2021) The neural resource allocation problem when enhancing human bodies with extra robotic limbs. *Nat Mach Intell* 3:850–860.
- Ejaz N, Hamada M, Diedrichsen J (2015) Hand use predicts the structure of representations in sensorimotor cortex. *Nat Neurosci* 18:1034–1040 Available at: <http://www.nature.com/articles/nn.4038>.
- Fischl B, Liu a, Dale a M (2001) Automated manifold surgery: constructing geometrically accurate and topologically correct models of the human cerebral cortex. *IEEE Trans Med Imaging* 20:70–80 Available at: <http://www.ncbi.nlm.nih.gov/pubmed/11293693>.
- Fischl B, Rajendran N, Busa E, Augustinack J, Hinds O, Yeo BTT, Mohlberg H, Amunts K, Zilles K (2008) Cortical folding patterns and predicting cytoarchitecture. *Cereb Cortex* 18:1973–1980.
- Fling BW, Benson BL, Seidler RD (2013) Transcallosal sensorimotor fiber tract structure-function relationships. *Hum Brain Mapp* 34:384–395 Available at: <https://onlinelibrary.wiley.com/doi/10.1002/hbm.21437>.
- Flor H, Elbert T, Knecht S, Wienbruch C, Pantev C, Birbaumers N, Larbig W, Taub E (1995) Phantom-limb pain as a perceptual correlate of cortical reorganization following arm amputation. *Nature* 375:482–484.
- Fouad MM, Amin KM, El-Bendary N, Hassanien AE (2015) Brain Computer Interface: A Review. In: *Brain-Computer Interfaces* (Hassanien AE, Azar AT, eds), pp 3–30 Intelligent Systems Reference Library. Cham: Springer International Publishing. Available at: [https://link.springer.com/10.1007/978-3-319-10978-7\\_1](https://link.springer.com/10.1007/978-3-319-10978-7_1).
- Glasser MF, Coalson TS, Robinson EC, Hacker CD, Harwell J, Yacoub E, Ugurbil K, Andersson J, Beckmann CF, Jenkinson M, Smith SM, Van Essen DC (2016) A multi-modal parcellation of

human cerebral cortex. *Nature* 536:171–178 Available at:  
<http://www.nature.com/doi/10.1038/nature18933>.

Graziano MSA, Aflalo TN (2007) Mapping behavioral repertoire onto the cortex. *Neuron* 56:239–251.

Haber WB (1955) Effects of Loss of Limb on Sensory Functions. *J Psychol* 40:115–123 Available at:  
<http://www.tandfonline.com/doi/abs/10.1080/00223980.1955.9712969>.

Hahamy A, Macdonald SN, van den Heiligenberg F, Kieliba P, Emir U, Malach R, Johansen-Berg H, Brugger P, Culham JC, Makin TR (2017) Representation of Multiple Body Parts in the Missing-Hand Territory of Congenital One-Handers. *Curr Biol* 27:1350–1355 Available at:  
<http://dx.doi.org/10.1016/j.cub.2017.03.053>.

Hahamy A, Makin TR (2019) Remapping in Cerebral and Cerebellar Cortices Is Not Restricted by Somatotopy. *J Neurosci* 39:9328–9342 Available at:  
<https://www.jneurosci.org/lookup/doi/10.1523/JNEUROSCI.2599-18.2019>.

Hahamy A, Sotiropoulos SN, Henderson Slater D, Malach R, Johansen-Berg H, Makin TR (2015) Normalisation of brain connectivity through compensatory behaviour, despite congenital hand absence. *Elife* 4:1–12 Available at: <https://elifesciences.org/articles/04605>.

Hamzei F, Liepert J, Dettmers C, Adler T, Kiebel S, Rijntjes M, Weiller C (2001) Structural and functional cortical abnormalities after upper limb amputation during childhood. *Neuroreport* 12:957–962.

Heming EA, Cross KP, Takei T, Cook DJ, Scott SH (2019) Independent representations of ipsilateral and contralateral limbs in primary motor cortex. *Elife* 8:1–26.

Jenkinson M, Bannister P, Brady M, Smith S (2002) Improved Optimization for the Robust and Accurate Linear Registration and Motion Correction of Brain Images. *Neuroimage* 17:825–841.

Jenkinson M, Beckmann CF, Behrens TEJ, Woolrich MW, Smith SM (2012) FSL. *Neuroimage* 62:782–790 Available at: <https://linkinghub.elsevier.com/retrieve/pii/S1053811911010603>.

Kambi N, Halder P, Rajan R, Arora V, Chand P, Arora M, Jain N (2014) Large-scale reorganization of the somatosensory cortex following spinal cord injuries is due to brainstem plasticity. *Nat Commun* 5:3602 Available at: <http://www.nature.com/articles/ncomms4602>.

Katz D (1920) Psychologische versuche mit amputierten, *Z. Psychol.* Barth.

Kellner E, Dhital B, Kiselev VG, Reiser M (2016) Magnetic Resonance in Med - 2015 - Kellner - Gibbs-ringing artifact removal based on local subvoxel-shifts.pdf. *Magn Reson Med* 76:1574–1581.

Kew JJM, Ridding MC, Rothwell JC, Passingham RE, Leigh PN, Sooriakumaran S, Frackowiak RSJ, Brooks DJ (1994) Reorganization of cortical blood flow and transcranial magnetic stimulation maps in human subjects after upper limb amputation. *J Neurophysiol* 72:2517–2524.

Kikkert S, Kolasinski J, Jbabdi S, Tracey I, Beckmann CF, Berg HJ, Makin TR (2016) Revealing the neural fingerprints of a missing hand. *Elife* 5:1–19.

Kriegeskorte N, Mur M, Bandettini P (2008) Representational similarity analysis - connecting the branches of systems neuroscience. *Front Syst Neurosci* 2:4 Available at:  
<http://www.pubmedcentral.nih.gov/articlerender.fcgi?artid=2605405&tool=pmcentrez&rendertype=abstract> [Accessed July 13, 2012].

Leemans A, Jeurissen B, Sijbers J (2009) ExploreDTI : a graphical toolbox for processing. :5–6.

Levelt CN, Hübener M (2012) Critical-period plasticity in the visual cortex. *Annu Rev Neurosci*

35:309–330.

- Lissek S, Wilimzig C, Stude P, Pleger B, Kalisch T, Maier C, Peters SA, Nicolas V, Tegenthoff M, Dinse HR (2009) Immobilization Impairs Tactile Perception and Shrinks Somatosensory Cortical Maps. *Curr Biol* 19:837–842.
- Maimon-Mor RO, Schone HR, Slater DH, Faisal AA, Makin TR (2021) Early life experience sets hard limits on motor learning as evidenced from artificial arm use. *Elife* 10:1–26.
- Makin TR (2021) Phantom limb pain: Thinking outside the (mirror) box. *Brain* 144:1929–1932.
- Makin TR, Cramer AO, Scholz J, Hahamy A, Slater DH, Tracey I, Johansen-Berg H (2013a) Deprivation-related and use-dependent plasticity go hand in hand. *Elife* 2:1–15.
- Makin TR, Flor H (2020) Brain (re)organisation following amputation: Implications for phantom limb pain. *Neuroimage* 218:116943 Available at: <https://doi.org/10.1016/j.neuroimage.2020.116943>.
- Makin TR, Scholz J, Filippini N, Henderson Slater D, Tracey I, Johansen-Berg H (2013b) Phantom pain is associated with preserved structure and function in the former hand area. *Nat Commun* 4:1570–1578 Available at: <http://dx.doi.org/10.1038/ncomms2571>.
- Merzenich MM, Nelson RJ, Stryker MP, Cynader MS, Schoppmann A, Zook JM (1984) Somatosensory cortical map changes following digit amputation in adult monkeys. *J Comp Neurol* 224:591–605 Available at: <http://doi.wiley.com/10.1002/cne.902240408>.
- Muret D, Makin TR (2021) The homeostatic homunculus: rethinking deprivation-triggered reorganisation. *Curr Opin Neurobiol* 67:115–122 Available at: <https://doi.org/10.1016/j.conb.2020.08.008>.
- O’Boyle DJ, Moore CEG, Poliakoff E, Butterworth R, Sutton A, Cody FWJ (2001) Human locognosic acuity on the arm varies with explicit and implicit manipulations of attention: Implications for interpreting elevated tactile acuity on an amputation stump. *Neurosci Lett* 305:37–40.
- Ogawa K, Mitsui K, Imai F, Nishida S (2019) Long-term training-dependent representation of individual finger movements in the primary motor cortex. *Neuroimage* 202:116051 Available at: <http://www.ncbi.nlm.nih.gov/pubmed/31351164> [Accessed November 16, 2021].
- Philip BA, Buckon C, Sienko S, Aiona M, Ross S, Frey SH (2015) Maturation and experience in action representation: Bilateral deficits in unilateral congenital amelia. *Neuropsychologia* 75:420–430.
- Philip BA, Frey SH (2011) Preserved grip selection planning in chronic unilateral upper extremity amputees. *Exp Brain Res* 214:437–452.
- Philip BA, Frey SH (2014) Compensatory Changes Accompanying Chronic Forced Use of the Nondominant Hand by Unilateral Amputees. *J Neurosci* 34:3622–3631 Available at: <https://www.jneurosci.org/lookup/doi/10.1523/JNEUROSCI.3770-13.2014>.
- Pons TP, Garraghty PE, Ommaya AK, Kaas JH, Taub E, Mishkin M (1991) Massive Cortical Reorganization After Sensory Deafferentation in Adult Macaques. *Science (80- )* 252:1857–1860 Available at: <http://www.sciencemag.org/cgi/doi/10.1126/science.1843843>.
- Postans M, Parker GD, Lundell H, Ptito M, Hamandi K, Gray WP, Aggleton JP, Dyrby TB, Jones DK, Winter M (2020) Uncovering a Role for the Dorsal Hippocampal Commissure in Recognition Memory. *Cereb Cortex* 30:1001–1015.
- Pruszynski JA, Johansson RS, Flanagan JR (2016) A rapid tactile-motor reflex automatically guides reaching toward handheld objects. *Curr Biol* 26:788–792 Available at:

<http://dx.doi.org/10.1016/j.cub.2016.01.027>.

- R Core Team (2022) R: A language and environment for statistical computing. Accessed 1st April 2019 Available at: <https://www.r-project.org/>.
- Raffin E, Mattout J, Reilly KT, Giroux P (2012) Disentangling motor execution from motor imagery with the phantom limb. *Brain* 135:582–595.
- Raffin E, Richard N, Giroux P, Reilly KT (2016) Primary motor cortex changes after amputation correlate with phantom limb pain and the ability to move the phantom limb. *Neuroimage* 130:134–144.
- Raja Beharelle A, Dick AS, Josse G, Solodkin A, Huttenlocher PR, Levine SC, Small SL (2010) Left hemisphere regions are critical for language in the face of early left focal brain injury. *Brain* 133:1707–1716.
- Ramachandran VS, Altschuler EL (2009) The use of visual feedback, in particular mirror visual feedback, in restoring brain function. *Brain* 132:1693–1710.
- Schieber MH (2001) Constraints on Somatotopic Organization in the Primary Motor Cortex. *J Neurophysiol* 86:2125–2143 Available at: <https://www.physiology.org/doi/10.1152/jn.2001.86.5.2125>.
- Schieber MH, Hibbard LS (1993) How somatotopic is the motor cortex hand area? *Science* (80-) 261:489–492.
- Simões EL, Bramati I, Rodrigues E, Franzoi A, Moll J, Lent R, Tovar-Moll F (2012) Functional expansion of sensorimotor representation and structural reorganization of callosal connections in lower limb amputees. *J Neurosci* 32:3211–3220.
- Smith SM, Jenkinson M, Johansen-Berg H, Rueckert D, Nichols TE, Mackay CE, Watkins KE, Ciccarelli O, Cader MZ, Matthews PM, Behrens TEJ (2006) Tract-based spatial statistics: Voxelwise analysis of multi-subject diffusion data. *Neuroimage* 31:1487–1505.
- Smith SM, Jenkinson M, Woolrich MW, Beckmann CF, Behrens TEJ, Johansen-Berg H, Bannister PR, De Luca M, Drobnjak I, Flitney DE, Niazy RK, Saunders J, Vickers J, Zhang Y, De Stefano N, Brady JM, Matthews PM (2004) Advances in functional and structural MR image analysis and implementation as FSL. *Neuroimage* 23:208–219.
- Soteropoulos DS, Edgley SA, Baker SN (2011) Lack of evidence for direct corticospinal contributions to control of the ipsilateral forelimb in monkey. *J Neurosci* 31:11208–11219.
- Sur M, Rubenstein JLR (2005) Patterning and Plasticity of the Cerebral Cortex. *Science* (80-) 310:805–810 Available at: <https://onlinelibrary.wiley.com/doi/10.1002/9780470015902.a0000090.pub2>.
- Takesian AE, Hensch TK (2013) Balancing plasticity/stability across brain development. In: *Progress in Brain Research*, 1st ed., pp 3–34. Elsevier B.V. Available at: <http://dx.doi.org/10.1016/B978-0-444-63327-9.00001-1>.
- Teuber, H and Krieger, HP and Bender M (1949) Reorganization of sensory function in amputation stumps: 2-point discrimination. *Fed Proc* 8:156--156.
- Tillema JM, Byars AW, Jacola LM, Schapiro MB, Schmithorst VJ, Szaflarski JP, Holland SK (2008) Cortical reorganization of language functioning following perinatal left MCA stroke. *Brain Lang* 105:99–111.
- Tournier JD, Smith R, Raffelt D, Tabbara R, Dhollander T, Pietsch M, Christiaens D, Jeurissen B, Yeh

- CH, Connelly A (2019) MRtrix3: A fast, flexible and open software framework for medical image processing and visualisation. *Neuroimage* 202:116137 Available at: <https://doi.org/10.1016/j.neuroimage.2019.116137>.
- Tuckute G, Paunov A, Kean H, Small H, Mineroff Z, Blank I, Fedorenko E (2022) Frontal language areas do not emerge in the absence of temporal language areas: A case study of an individual born without a left temporal lobe. *Neuropsychologia* 169:108184 Available at: <https://doi.org/10.1016/j.neuropsychologia.2022.108184>.
- Valyear KF, Philip BA, Cirstea CM, Chen PW, Baune NA, Marchal N, Frey SH (2020) Interhemispheric transfer of post-amputation cortical plasticity within the human somatosensory cortex. *Neuroimage* 206:116291 Available at: <https://doi.org/10.1016/j.neuroimage.2019.116291>.
- Vega-Bermudez F, Johnson KO (2002) Spatial acuity after digit amputation. *Brain* 125:1256–1264.
- Veraart J, Novikov DS, Christiaens D, Ades-aron B, Sijbers J, Fieremans E (2016) Denoising of diffusion MRI using random matrix theory. *Neuroimage* 142:394–406 Available at: <http://dx.doi.org/10.1016/j.neuroimage.2016.08.016>.
- Verstynen T, Diedrichsen J, Albert N, Aparicio P, Ivry RB (2005) Ipsilateral Motor Cortex Activity During Unimanual Hand Movements Relates to Task Complexity. *J Neurophysiol* 93:1209–1222 Available at: <https://www.physiology.org/doi/10.1152/jn.00720.2004>.
- Vos SB, Tax CMW, Luijten PR, Ourselin S, Leemans A, Froeling M (2017) The importance of correcting for signal drift in diffusion MRI. *Magn Reson Med* 77:285–299.
- Walther A, Nili H, Ejaz N, Alink A, Kriegeskorte N, Diedrichsen J (2016) Reliability of dissimilarity measures for multi-voxel pattern analysis. *Neuroimage* 137:188–200 Available at: <http://dx.doi.org/10.1016/j.neuroimage.2015.12.012>.
- Waters-Metenier S, Husain M, Wiestler T, Diedrichsen J (2014) Bihemispheric transcranial direct current stimulation enhances effector-independent representations of motor synergy and sequence learning. *J Neurosci* 34:1037–1050.
- Waters S, Wiestler T, Diedrichsen J (2017) Cooperation not competition: Bihemispheric tDCS and fMRI show role for ipsilateral hemisphere in motor learning. *J Neurosci* 37:7500–7512.
- Werhahn KJ, Mortensen J, Kaelin-Lang A, Boroojerdi B, Cohen LG (2002) Cortical excitability changes induced by deafferentation of the contralateral hemisphere. *Brain* 125:1402–1413.
- Wesselink DB, van den Heiligenberg FM, Ejaz N, Dempsey-Jones H, Cardinali L, Tarall-Jozwiak A, Diedrichsen J, Makin TR (2019) Obtaining and maintaining cortical hand representation as evidenced from acquired and congenital handlessness. *Elife* 8:1–19 Available at: <https://elifesciences.org/articles/37227>.
- Wetzels R, Matzke D, Lee MD, Rouder JN, Iverson GJ, Wagenmakers EJ (2011) Statistical evidence in experimental psychology: An empirical comparison using 855 t tests. *Perspect Psychol Sci* 6:291–298.
- Wiestler T, Diedrichsen J (2013) Skill learning strengthens cortical representations of motor sequences. *Elife* 2:1–20 Available at: <https://elifesciences.org/articles/00801>.
- Yousry TA, Schmid UD, Alkadhi H, Schmidt D, Peraud A, Buettner A, Winkler P (1997) Localization of the motor hand area to a knob on the precentral gyrus. A new landmark. *Brain* 120:141–157.
- Yu WS, van Duinen H, Gandevia SC (2010) Limits to the Control of the Human Thumb and Fingers in Flexion and Extension. *J Neurophysiol* 103:278–289 Available at: <https://www.physiology.org/doi/10.1152/jn.00797.2009>.

## Figure captions

**Figure 1. Intact hand motor performance.** Schematic representation of the finger configurations used for the motor task during the **(A)** training and **(D)** fMRI sessions. The colours represent the graded difficulty across configurations (based on the inter-finger enslavement components), with colder colours indicating more difficult configurations. **(B, E)** Line plots of the mean deviance values ( $\pm$  SEM) across blocks/runs for the (B) training and (D) fMRI sessions. Deviance scores reflect the extent to which the pressure exerted by the 5 fingers deviated from the expected configuration (see *General procedure* in the method section). Smaller deviance reflects better performance. **(C, F)** Effect plots showing the marginal means of the deviation values predicted by the model (repeated measures ANCOVA, controlling for age) for the (C) training and (F) fMRI session, as well as individual participants performance (grey dots). For the training session (C), deviance was averaged over the easy configurations (345, 123, and 124) and difficult configurations (245 and 135), for the first and last blocks each participant performed. For the fMRI session (F), deviance was averaged over the easy (145 and 234) and difficult (134, 125, and 235) configurations, for the first and 4th run. In the training session, participants showed improvement in motor control, as indicated by a decrease in deviance, but one-handers demonstrated reduced learning for the most challenging configurations. In the fMRI session, both one-handers and controls showed reduced performance, relative to controls.

**Figure 2. BA3b ROI.** Amputees showed significantly larger activity than the control and one-hander groups in the ipsilateral cortex for the difficulty condition (Panel B) but this did not result in an increased information content (Panel C). **A)** Bilateral hand BA3b ROIs used in the analyses (one example participant). **B)** Brain activity (zscores) in the contralateral and ipsilateral hemispheres averaged across runs and across easy and difficult configurations. **C)** Information content (dissimilarities between configuration pairs) in the contralateral and ipsilateral hemispheres averaged across runs. Only the dissimilarities between the easiest (e.g., the green square in Figure 3A) and most difficult (e.g., the blue square in Figure 3A) finger configurations were selected. The unshaded dots with different colours represent individual participants. Colour filled dots with asterisks at the top of plots B and C indicate significant difference (Bonferroni corrected) between the groups specified by the colours in a specific or averaged condition. Lines with asterisks refer to significant difference (Bonferroni corrected) between conditions within a group. We are reporting here only the relevant comparisons, for the complete analysis, please refer to the results section.

**Figure 3. Functional homotopy and contralateral typicality in multivariate representational structure.** **A)** Representation dissimilarity matrices (RDMs) across multi-finger configurations, groups and hemispheres. Colours reflect crossnobis distance, with warmer distances showing greater pairwise dissimilarity. The green and blue squares on the top left RDM highlight the easiest (green) and most difficult (blue) finger configuration pairs, respectively for the analysis in Figure 2C (the same pairs were used for the other RDMs). The dashed area on the Contralateral Controls RDM indicate the typical contralateral representation used to assess the typicality of representation in Figure 3C. **B)** Inter-hemispheric correlation ( $\rho$ ) between the contralateral and ipsilateral RDM within individuals was used to calculate homotopy. **C)** The individual RDMs of the amputees and one-handers groups were correlated with the average contralateral RDM of the controls (the typical contralateral representation) to calculate contra-typical representation. All other annotations are as reported in Figure legend 2. Amputees showed typical contralateral representational motifs in their missing hand cortex for representing multi-finger configurations with their intact hand.

**Figure 4. M1 and hMT+ ROIs.** We extended our analyses from BA3b (Figure 2) to explore **A) M1** and **D) hMT+**. In the case of univariate analysis, unlike BA3b, we did not find a three-way interaction in either **B) M1** or **E) hMT+**. Specifically, the increase in averaged activity related to task difficulty, which we observed in the ipsilateral hemisphere of the amputees (Figure 2B), was not evident in these control ROIs. In M1, there was a general increase in averaged activity related to difficulty across all groups, but this effect was seen only in the contralateral hemisphere (Panel B). Additionally, we noted a significant interaction between group and hemisphere in M1, indicating that the difference in activity between the two hemispheres was reduced in amputees compared to the control groups. We did not identify any significant main effects or interactions in hMT+ (Panel E). For the multivariate analysis, in **C) M1**, we observed a similar decrease in distance with increasing difficulty across groups and hemispheres, mirroring what we found in BA3b (Figure 2C). However, in contrast to BA3b, there was no main effect of group in M1. Lastly, in **F) hMT+**, our analyses did not reveal any significant main effects or interactions.

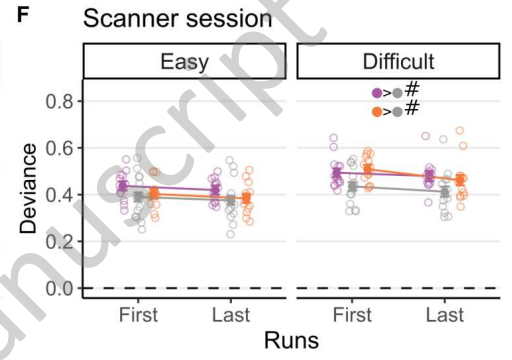
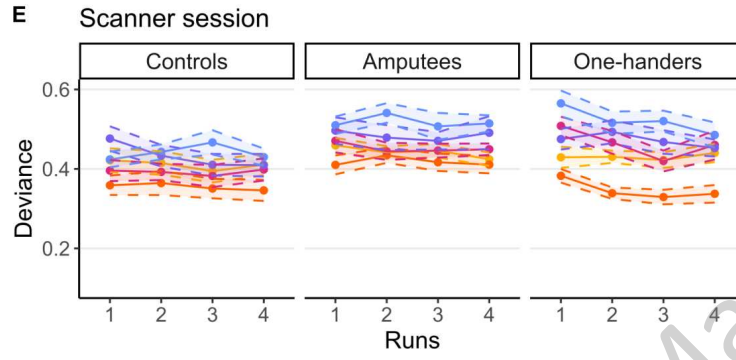
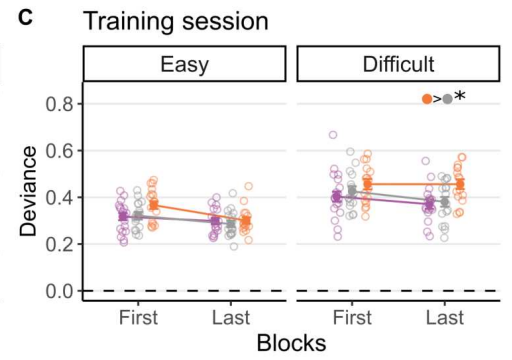
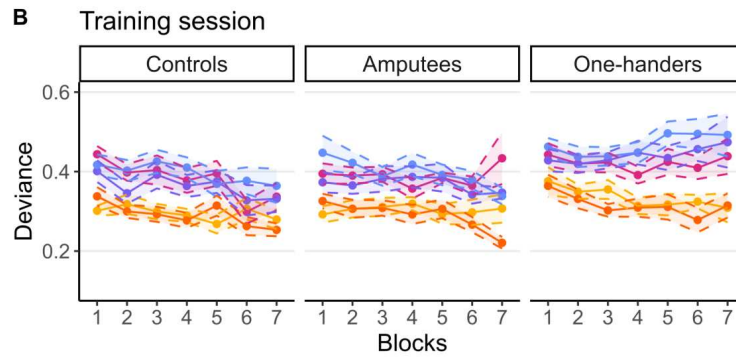


## Tables

Table 1

Table 1. All participants

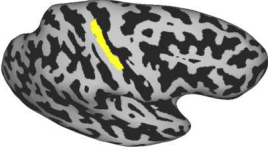
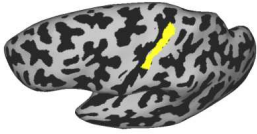
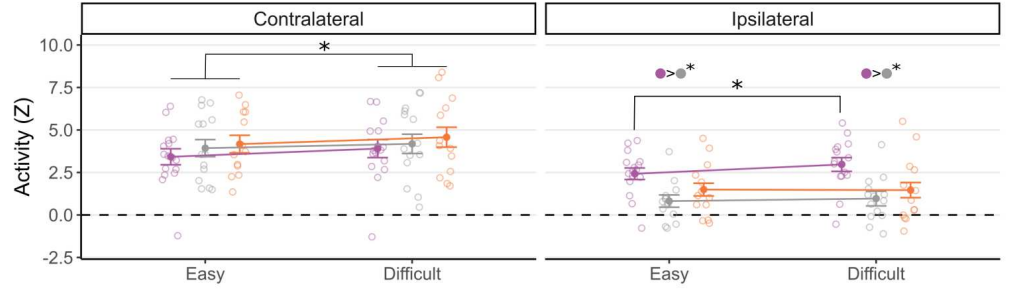
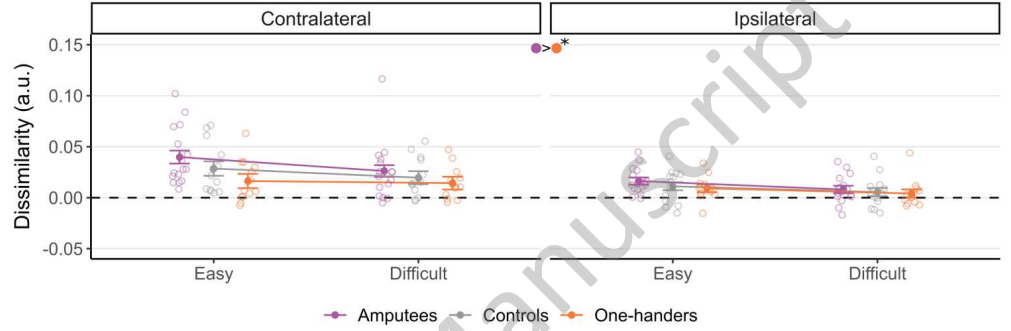
ID	Group	Gender	Age	Affected Side	Handedness	Lost Dominant Hand	Years Without Hand
MA02	One-handers	M	39	Left	Right	0	39
MA03	One-handers	M	35	Right	Left	0	35
MA05	One-handers	F	29	Left	Right	0	29
MA08	One-handers	M	58	Left	Right	0	58
MA11	One-handers	F	37	Right	Left	0	37
MA12	One-handers	F	52	Left	Right	0	52
MA14	One-handers	M	32	Left	Right	0	32
MA16	One-handers	M	61	Left	Right	0	61
MA18	One-handers	F	42	Left	Right	0	42
MA21	One-handers	F	53	Right	Left	0	53
MA25	One-handers	F	29	Left	Right	0	29
MA26	One-handers	M	44	Left	Right	0	44
MA28	One-handers	M	35	Right	Left	0	35
MA29	One-handers	F	35	Right	Left	0	35
MA30	One-handers	F	51	Left	Right	0	51
MA34	One-handers	F	63	Right	Left	0	63
MA01	Amputees	M	42	Right	Left	0	15
MA04	Amputees	M	51	Left	Right	0	32
MA06	Amputees	M	38	Left	Right	0	11
MA07	Amputees	M	49	Left	Right	0	32
MA09	Amputees	F	25	Right	Left	0	7
MA10	Amputees	M	69	Right	Left	0	16
MA13	Amputees	M	44	Right	Left	0	18
MA15	Amputees	M	54	Left	Right	0	26
MA17	Amputees	M	62	Left	Right	0	31
MA19	Amputees	M	56	Left	Right	0	2
MA20	Amputees	M	26	Left	Right	0	8
MA22	Amputees	M	55	Right	Right	1	29
MA23	Amputees	F	48	Left	Right	0	1
MA24	Amputees	M	50	Right	Right	1	27
MA27	Amputees	M	66	Right	Right	1	26
MA31	Amputees	F	37	Right	Left	0	6
MA32	Amputees	M	56	Left	Right	0	12
MA33	Amputees	F	44	Left	Right	0	14
MA35	Amputees	M	60	Left	Right	0	1
MC03	Controls	M	29	NA	Left	NA	NA
MC04	Controls	F	24	NA	Right	NA	NA
MC05	Controls	M	52	NA	Right	NA	NA
MC06	Controls	M	47	NA	Left	NA	NA
MC07	Controls	F	39	NA	Right	NA	NA
MC08	Controls	M	32	NA	Left	NA	NA
MC09	Controls	M	53	NA	Left	NA	NA
MC10	Controls	F	38	NA	Left	NA	NA
MC11	Controls	F	67	NA	Right	NA	NA
MC12	Controls	M	41	NA	Right	NA	NA
MC13	Controls	M	48	NA	Ambi	NA	NA
MC14	Controls	M	42	NA	Right	NA	NA
MC15	Controls	M	41	NA	Right	NA	NA
MC17	Controls	M	51	NA	Right	NA	NA
MC19	Controls	F	45	NA	Left	NA	NA
MC22	Controls	F	63	NA	Right	NA	NA
MC23	Controls	F	43	NA	Left	NA	NA



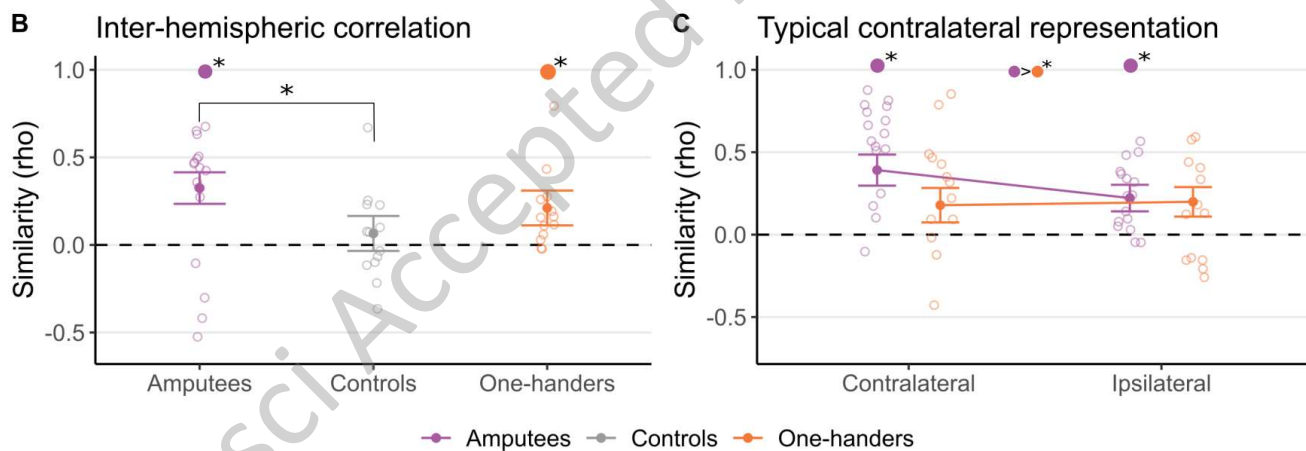
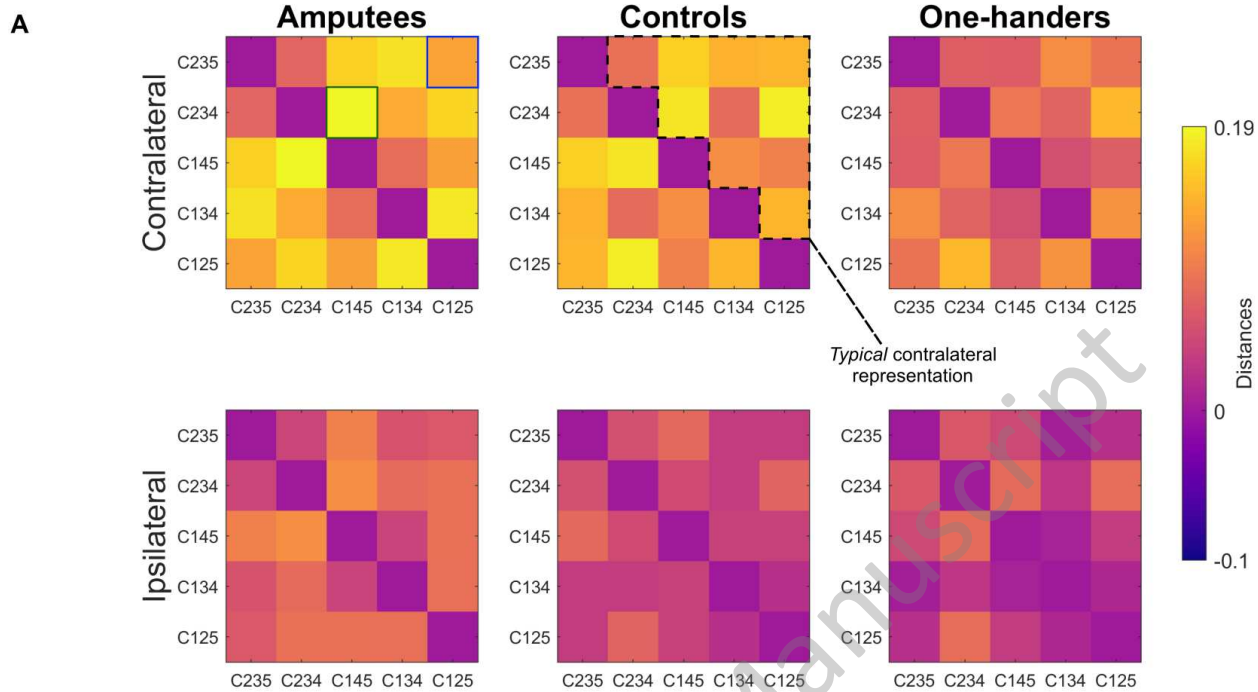
1 2 3 4 5

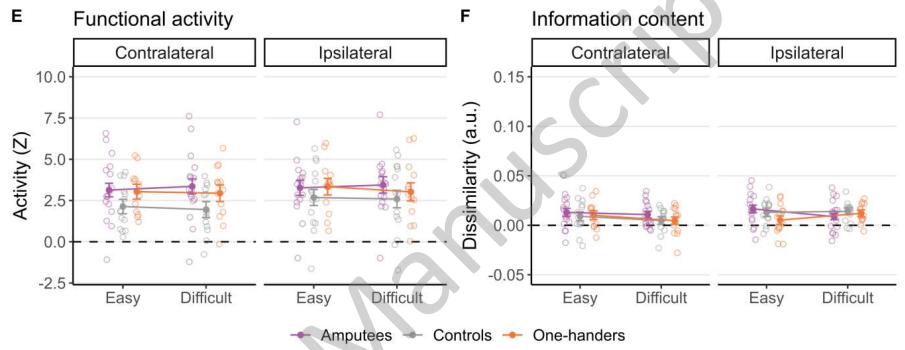
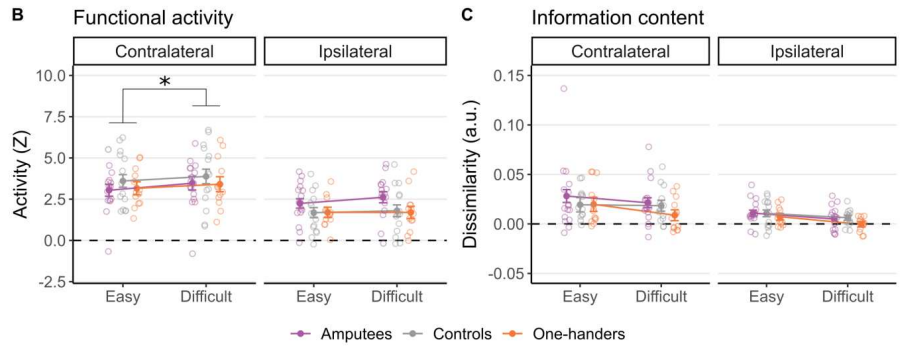
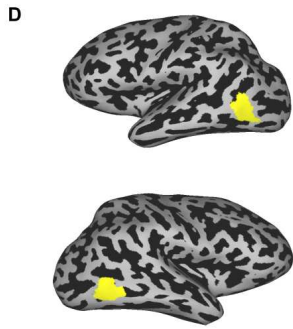
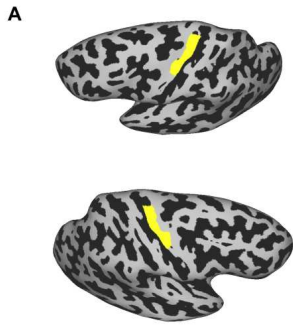
Amputees Controls One-handers

JNeurosci Accepted Manuscript

**A****B** Functional activity**C** Information content

JNeurosci Accepted Manuscript





JNeurosci Accepted Manuscript